Full Title: Protein Arginine Methyltransferase 5 (PRMT5) selective inhibitors suppress inflammatory T cell responses and Experimental Autoimmune Encephalomyelitis

Running title: PRMT5 drives inflammatory T cell responses and autoimmunity

Authors: Lindsay M. Webb[†#], Stephanie A. Amici[†], Kyle Jablonski[†], Himanshu Savardekar[†], Amanda R. Panfil[‡], Linsen Li[§], Wei Zhou[§], Kevin Peine[^], Vrajesh Karkhanis[¶], Eric Bachelder[^], Kristy Ainslie[^], Patrick L. Green[‡], Chenglong Li[§], Robert A. Baiocchi[¶] and Mireia Guerau-de-Arellano[†||]

Affiliation

[†] Division of Medical Laboratory Science, School of Health and Rehabilitation Sciences, College of Medicine, The Ohio State University, Columbus, OH 43210

[‡] College of Veterinary Medicine, The Ohio State University, Columbus, OH 43210

[§] Division of Medicinal Chemistry and Pharmacology, College of Pharmacy, The Ohio State University, Columbus OH 43210

[¶] Division of Hematology, Department of Internal Medicine, College of Medicine, The Ohio State University Wexner Medical Center

[^]Division of Molecular Pharmaceutics, Eshelman School of Pharmacy, University of North Carolina Chapel Hill

[‡]Biomedical Sciences Graduate Program, College of Medicine, The Ohio State University

[||]corresponding author

Keywords: memory T cell, proliferation, PRMT5, arginine methylation, autoimmunity, Experimental Autoimmune Encephalomyelitis

Corresponding author:

Mireia Guerau-de-Arellano, PharmD PhD. The Ohio State University School of Health and Rehabilitation Sciences- Division of Medical Laboratory Science. Atwell Hall 535; 453 W 10th Ave. Columbus (OH) 43210 USA. E-mail: mireia.guerau@osumc.edu; Tel: 614 293 4176; Fax: 614 292 0210

Abbreviations

DTH: Delayed-Type Hypersensitivity

EAE: Experimental Autoimmune Encephalomyelitis

MBP: Myelin Basic Protein

MOG: Myelin Oligodendrocyte Glycoprotein

PRMT: Protein Arginine Methyl Transferase

SAM: (S)-AdenosylMethionine

Funding

This work was supported by funds from Drug Development Institute at The Ohio State University Comprehensive Cancer Center (M.G-de-A., R.A.B., C.L), NIH NIAID R01AI121405 (M.G-de-A), The Leukemia Lymphoma Society Translational Research Program (R.A.B., C.L) start-up funds (M. G-de-A.) and the Comprehensive Cancer Center Medicinal Chemistry Shared Resource (CCC core grant CCSG: P30CA016058).

Copyright Information

This is the accepted, uncopyedited version of the manuscript. The definitive version was published in *The Journal of Immunology* Vol 198: 1-14. DOI: doi:10.4049/jimmunol.1601702.

Abstract

In the autoimmune disease multiple sclerosis (MS) and its animal model Experimental Autoimmune Encephalomyelitis (EAE), expansion of pathogenic, myelin-specific Th1 cell populations drives active disease; selectively targeting this process may be the basis for a new therapeutic approach. Previous studies have hinted a role for protein arginine methylation in immune responses, including T cell-mediated autoimmunity and EAE. However, a conclusive role for the Protein Arginine Methyl Transferase (PRMT) enzymes that catalyze these reactions has been lacking. PRMT5 is the main PRMT responsible for symmetric dimethylation of arginine residues of histones and other proteins. PRMT5 drives embryonic development and cancer, but its role in T cells, if any, has not been investigated. Here, we show that PRMT5 is an important modulator of $CD4^+$ T cell expansion. PRMT5 was transiently up-regulated during maximal proliferation of both mouse and human memory Th cells. PRMT5 expression was regulated upstream by the NF-κB pathway, and it promoted IL-2 production and proliferation. Blocking PRMT5 with novel, highly selective small molecule PRMT5 inhibitors severely blunted memory Th expansion, with preferential suppression of Th1 over Th2 cells. *In vivo,* PRMT5 blockade efficiently suppressed recall T cell responses and reduced inflammation in Delayed Type Hypersensitivity (DTH) and clinical disease in Experimental Autoimmune Encephalomyelitis (EAE) mouse models. These data implicate PRMT5 in regulation of adaptive memory T helper cell responses and suggest PRMT5 inhibitors may be a novel therapeutic approach for T cell-mediated inflammatory disease.

1. **Introduction**

Multiple Sclerosis (MS) is a chronic inflammatory disease of the central nervous system that affects 2 million young adults worldwide (1). MS is driven by myelin-reactive inflammatory T cells, resulting in axonal demyelination and disability (2). The reactivation and expansion of myelin-specific inflammatory T cells is associated with active MS disease, including relapses (3-8). Drugs that suppress these processes may therefore prevent or curtail the spread of this devastating disease.

MS is associated with both increased Th1 and Th17 inflammatory responses (9) and deficient Th2 and Treg responses (10). In particular, an imbalance between reciprocal Th1 and Th2 responses has been reported as an important etiologic factor in MS. Several studies have shown that T cells from MS patients favor the pro-inflammatory Th1 phenotype as opposed to a Th2 phenotype (11-13). Furthermore, although myelin-reactive T cells are present in healthy individuals, MS patients have increased frequencies of myelin-specific T cells with an activated memory phenotype (14-16).

Upon re-exposure to antigen, memory T cells multiply quickly, providing a large army of responding T cells. TCR stimulation results in the activation of several signaling pathways, including Notch, c-myc, NFAT, ERK, JNK, NF-kB and mTOR pathways (17). Nuclear translocation of NFAT, Oct, NF-kB and AP-1 transcription factors activate transcription of the pro-proliferative cyokine IL-2 (18). In addition, Notch and c-myc induce T cell proliferation (19), whereas the mTOR pathway is essential for glucose metabolism in proliferating T cells (20). Memory T cells transition quickly from a non-proliferative resting state to maximal proliferation 2-4 days after antigen exposure. This is followed by a return to a resting state 7-10 days later (21). Although this process is essential in the immune response against bacterial and other infections, memory T cell expansion in response to self-antigens can be harmful, resulting in excessive inflammation and autoimmunity.

What role, if any, arginine methylation plays in this process remains vastly unexplored. However, previous studies provide some clues for further investigation. A role for methylation in physiologic immune responses was first suggested by the clinical signs of a debilitating immunodeficiency observed in adenosine deaminase (ADA)-deficient patients (22, 23). In ADA, the accumulation of adenosine and deoxyadenosine inhibits S-adenosyl methionine (SAM)-dependent methylation reactions (23, 24). In particular, TCR/CD28-mediated proliferation and cytokine production are inhibited in ADA deficient patients (22, 23). Similarly, global methyltransferase inhibitors have been shown to have strong immunosuppressive properties and abrogate T cell-mediated autoimmunity (25-28). Methylthioadenosine (MTA), a physiological methyl-donor substrate for methylation reactions, can also act as a methylation inhibitor when present at high concentrations (27). It has been recently shown that alterations in the tumor environment result in high tumoral MTA levels that inhibit protein arginine methylation and suppress anti-cancer human T cell responses. Accumulating evidence therefore hints that the T cell effects of global methyltransferase inhibition are due to inhibition of Protein Arginine Methyl Transferases (PRMT) (29, 30). However, conclusive evidence demonstrating that PRMT are responsible for T cell suppression, as well as a specific role for the main symmetric dimethylation enzyme PRMT5, has been lacking.

PRMTs are a family of enzymes that catalyze arginine methylation of nucleosomal histones on chromatin and other proteins. Among PRMTs, type I PRMTs (PRMT1-4, 6 and 8) catalyze asymmetric dimethylation, while type II PRMTs (PRMT5 and 9) catalyze symmetric dimethylation at the ω-NH2 of arginine (31). Although PRMT9 can catalyze symmetric dimethylation of certain substrates, most SDM reactions of histones are catalyzed by PRMT5 (32). PRMT7 was considered a type II PRMT until recently but has been reclassified as a monomethylating Type III PRMT (33). The modifications catalyzed by PRMTs play a crucial role in a variety of cellular processes, from differentiation to signaling and proliferation (34). Among PRMTs, PRMT5 appears to play a particularly relevant role in the regulation of cell death and malignant transformation processes in mouse and humans (35-38). Indeed, PRMT5 is up-regulated in various human lymphoid malignancies (39-41) and solid tumors (42-48) and promotes cancer cell proliferation and survival (38, 46, 49, 50). This has led to the development of selective PRMT5-inhibiting drugs such as CMP5 and EPZ015666 as a potential new therapy in cancer (43, 51, 52). While PRMT5 is clearly involved in tumor growth and survival, its role in T cell responses and its impact on autoimmunity are unknown.

Here, we set out to investigate the role of PRMT5 activity in expansion of pathogenic Th1 cells that lead to MS. We found that PRMT5 transient up-regulation in response to TCR engagement *in vitro* is conserved in mouse and human memory Th1 and Th2 $CD4^+$ T cells. PRMT5 up-regulation in Th1 cells required NF-kB signaling, and inhibition of PRMT5 activity with PRMT5-selective inhibitors blunted IL-2 secretion and proliferative responses of memory Th cells. Interestingly, pathogenic Th1 cells were more sensitive to PRMT5 inhibition than benign Th2 cells, a desirable immunological profile for MS drugs. *In vivo,* treatment with the novel PRMT5 inhibitor HLCL65 suppressed antigen-specific T cell responses and inflammation in the DTH model of inflammation and EAE model of MS. This is the first evidence that PRMT5 plays an essential role in pathogenic Th1 cell responses. Further, we describe novel potent PRMT5 selective inhibitors that may provide a novel therapeutic strategy for Th1-mediated inflammatory autoimmune disease.

2. Materials and Methods.

2.1. Mice.

B10.PL (Jackson labs) and MBP TCR Tg mice (described by Dr. Goverman (53)) were bred in specific pathogen-free conditions at the OSU University Laboratory Animal Resources, under protocol # 2013A00000151. C57BL/6 and BALB/c mice were purchased from Taconic and Jackson laboratories, respectively.

2.2. Reagents.

PRMT5 inhibitor CMP5 was designed and synthesized at The Ohio State University as previously described (51). Briefly, the compound was designed to fit into the PRMT5 enzyme crystal structure, partially covering the binding pockets for both the methyl group donor, S-adenosylmethionine (SAM), and the acceptor protein arginine group. Stock CMP5 was dissolved in dimethylsulfoxide (DMSO) vehicle at a concentration of 100mM and further diluted to 25μM in DMSO for *in vitro* assays. PRMT5 inhibitor HLCL65 was dissolved in DMSO vehicle at a concentration of 50mM and was further diluted for in vitro assays. Stock Bay 11-7082 was dissolved in DMSO vehicle at a concentration of 10 mM. Bay 11 was further diluted at least 1:1000 for *in vitro* assays.

2.3. HLCL65-binding interaction prediction.

The crystal structure of human PRMT5:MEP50 complex (PDB ID: 4GQB) was used to predict the binding interaction of HLCL65 within the PRMT5 active site. The co-crystallized AdoMet analog (A9145C) and the histone H4 derived substrate peptide were deleted from the binding site. The small molecule ligand HLCL65 was prepared by Maestro (Schrödinger). Molecular docking was accomplished by Autodock4. The binding energy of the protein-ligand interaction in the shown binding mode was -13.14 kcal/mol.

2.4. Histone methyltransferase assays.

Histone methylation was performed using 2 μg of HeLa S3 core histones in the presence or absence of 15 μl of affinity-purified human SWItch/Sucrose Non Fermentable (hSWI/SNF) associated Flag-tagged PRMT5 or Flag-tagged PRMT7, as described previously (54). Reaction mixtures were spotted on Whatman P-81 filter paper, washed five times with 10 ml of 0.1 mm sodium carbonate buffer (pH 9.0) to remove unincorporated [3H]AdoMet, and methylated peptides were detected by scintillation counting.

2.5. Cells.

Mouse Th1 and Th2 cell lines were generated from Myelin Basic Protein (MBP) Ac1-11-specific T cell receptor (TCR) transgenic mice (53). Naïve T cells were isolated from TCR transgenic splenocytes by magnetic bead sorting using the $CD4^{+}CD62L^{+}$ isolation kit (Miltenyi Biotech) and activated with MBPAc1-11 (0.5 μg/ml) presented in irradiated splenocytes in Th1 (IL-12 + IFN-γ, anti-IL-4) or Th2 (IL-4, anti-IL-12 and anti-IFN-γ) conditions for two rounds. Th cell lines are not transformed and were therefore maintained by stimulation with MBPAc1-11 and irradiated splenocytes in the presence of recombinant IL-2 every 7-10 days. T cells collected 7-10 days after activation with MBPAc1-11 and irradiated splenocytes provided the resting Th cell condition. To avoid the presence of non-T cells in *in vitro* experiments, resting Th1 or Th2 cell lines were activated with anti-CD3/CD28 in the presence or absence of the PRMT5 inhibitors CMP5, HLCL65 or DMSO as vehicle control for various lengths of time indicated throughout the manuscript. Human Th1 and Th2 cells were generated by isolating CD4+ T cells with $CD4^{+}$ T cell isolation kit (Stem Cell Technologies) from human whole blood leukocytes from normal donors and activating on anti-CD3/CD28 Dynabeads (ThermoScientific) in Th1 or Th2 conditions (same as mouse) for 1 week. Th cells were then removed from the Dynabeads and reactivated with plate bound anti-CD3 (1ug/ml for Th1, 5ug/ml for Th2) and soluble CD28 (1ug/ml for Th1, 2ug/ml for Th2) for further experiments. Naïve $CD4^+$ T cells were isolated with the mouse naïve $CD4^+$ T cell isolation kit (Miltenyi) and activated with 5ug/ml coated anti-CD3 and 2ug/ml soluble anti-CD28. CCMCL1 cell lines are a mantle cell lymphoma cell line, described previously (55).

2.6. Western blot.

Cells were lysed in Passive Lysis Buffer (Promega) or RIPA buffer (10mM Tris, 150mM NaCl, 1% Triton X-100, 0.1% SDS, 1% deoxycholate) containing protease inhibitors and phosphatase inhibitors (Thermo Scientific). Protein concentrations were determined by Nanodrop 2000 or BCA assay (ThermoFisher). Equal quantities of protein (5-10 μg) were separated on 10-14% SDS-PAGE gels, and transferred to nitrocellulose or PVDF membranes (Biorad, 162-0177). Membranes were incubated with rabbit anti-PRMT5 (Abcam Ab31751, 1:500) antibody, anti-PRMT1 (CST 2449S), anti-PRMT7 (ab22110) or mouse anti-β-actin (Sigma, A1978 1:20000) antibody overnight at 4°C or for 3 hours at room temperature. After incubation with HRP-conjugated anti-rabbit (Sigma, A0545, 1:15000) or anti-mouse (Sigma, A9044 1:20000) antibody, Westerns were developed with SuperSignal West Pico Chemiluminescent Substrate (Thermo Scientific) and the luminescent signal was captured on film and developed on a Konica-Minolta SRX-101A or digitally on a Fuji LAS-4000 Imaging System. After incubation with fluorescently labeled anti-rabbit or anti-mouse secondary antibodies (Odyssey LI-COR), Western blots were imaged with Odyssey CLx. The western blotting bands were analyzed by ImageJ (Bio-Arts, Co. Ltd., Fukuoka, Japan) or ImageStudio software.

2.7. RNA isolation.

RNA was isolated with Trizol (Life Technologies) or the mirVana kit (Life Technologies) total RNA isolation protocol, according to manufacturer's instructions, and stored at -80^{0}C until analysis. RNA concentration and quality was determined using NanoDrop 2000.

2.8. Real-Time PCR.

For Real-Time PCR, 300-1000 ng of RNA from profiled samples were cDNA transcribed using random primers and Superscript II (Applied Biosystems) and Taqman Real-Time PCR was performed using m*Tbx21* (Mm00450960_m1) and m*HPRT* (Mm0044968_m1) primer sets (Life Technologies), according to manufacturer samples were cDNA transcribed using random primers and Superscript III (Applied Biosystems of similar amplification efficiency for test and control genes.) Initial denaturation step at 95°C for 10 minutes was followed by 40 cycles of denaturation at 95°C for 15 seconds and primer annealing/extension at 60°C for 60 seconds. Results were analyzed using the comparative Ct method.

2.9. Cytokine ELISA.

Cytokines were detected in supernatants at various points post-stimulation by a sandwich ELISA. Mouse IL-2 reagents were from BD, mouse IL-17 reagents were purchased from eBiosciences (Capture: 14-7175-85, Detection: 13-7177-85), human IL-2 reagents were purchased from Biolegend (Capture: 500302, Detection: 517605) and recombinant human IL-2 was purchased from Miltenyi. ELISA was performed as previously described (12).

2.10. ^{3}H-Thymidine Proliferation Assay.

Th1 and Th2 cell lines were plated on anti-CD3/CD28-coated wells (100,000 - 125,000 cells/well) and treated with CMP5 inhibitor, or vehicle control (DMSO) and/or increasing concentrations of IL-2 at the indicated concentrations. Two days after treatment, cells were pulsed with 1 µCi of tritiated-thymidine (^{3}H-thymidine). After 18 hours, cells were harvested on a Filtermate196 harvester (Packard/Perkin-Elmer, Waltham, MA, USA) and the amount of amount of ^{3}H-thymidine incorporated into the DNA was measured in a TopCount microplate scintillation and luminescence counter (Packard/Perkin-Elmer).

2.11. Intracellular flow cytometry.

On collection day, cells were treated with PMA/ionomycin and GolgiStop (BD Biosciences) for 4-6 hours and washed with FACS buffer prior to Fc region blockade and surface antibody staining (10 minutes, 4°C). Samples were then fixed with Fixation/Permeabilization buffer and washed with Permeabilization/Wash buffer (buffers from BD Biosciences, Cat# 554715). Intracellular proteins T-bet (Biolegend 644807), IL-17 (Biolegend 506916), and RORγt (eBiosciences 12-698880) were stained with the corresponding antibodies (T-bet clone: 4B10, IL-17 clone: TC11-18H10.1) and RORgt clone: AFKJS-9) for 30 minutes at 4 degrees. $CD4^{+}CD44^{+}$ T cells were gated on to analyze the $Tbet^{+}ROR\gamma t^{+}$, $IL\text{-}17^{+}ROR\gamma t^{+}$, and $Tbet^{+}IL\text{-}17^{+}$ double-positive populations.

2.12. shRNA lentivirus transfection and transduction.

Lentiviral vectors expressing five different PRMT5-targeted shRNAs (target set RHS4533-EG10419) and the universal negative control, pLKO.1 (RHS4080) were acquired from Open Biosystems. HEK293T cells (Takara Clontech) were transfected with lentiviral vectors plus DNA vectors encoding HIV Gag/Pol and VSV-G in 10cm dishes with Lipofectamine 2000 (Life Technologies), according to manufacturers instructions. Lentiviral particle-containing supernatant was collected after 72 hours, filtered through 0.45μm filters, and concentrated using ultracentrifugation in a Sorvall SW-41 swinging bucket rotor. Human Th1 cells were prepared by resuspending 500,000 cells in 50μl concentrated lentivirus plus 8μg/ml polybrene. Human Th1 cells were transduced by spinoculation at 2000xg for 2 hours at room temperature and then incubated for 1hr at 37 degrees. Virus was then washed out and cells were plated on anti-CD3/CD28 coated plates for proliferation or protein.

2.13. siRNA tranfection with Neon electroporation.

To knockdown PRMT5, we selected three siRNAs targeting different areas in the PRMT5 gene. Two siRNAs (namely, si#1 (5'-AAT TCC AAG GTG CAA TAG CGG CCT GTC TC-3), si#2 (5'-ACA CUU CAU AUG UCU GAG A-3') were synthesized in-house with the Silencer siRNA construction kit (Thermofisher AM1620M). The third siRNA (si#3) was purchased from Ambion (Cat # s77695). To transfect T cells, we used the Neon transfection system (Invitrogen) electroporation, following manufacturer's instructions and adapting them as indicated below. Human Th cells were prepared by washing twice with phosphate-buffered saline (PBS), removing all of the supernatant after the last wash. Five million primary T cells were ressuspended in 100µl of T buffer containing 1.5µg of siRNA and electroporated (1 pulse at 2100V for 20ms) using the Neon 100µl transfection pipette. Cells were mixed 1:1 with 100µl of 2% Viability Buffer (gift from Dr. Renzhi Han at OSU) to promote cell viability after electroporation. Finally, cells were plated into media lacking penicillin/streptomycin. Proliferation and protein expression were monitored as indicated in the text.

2.14. OVA-induced Delayed Type Hypersensitivity.

Complete Freund's Adjuvant (CFA) (Difco) and ovalbumin (OVA) emulsion was prepared at a 1:1 v/v ratio for a final concentration of 1500µg OVA per ml PBS. BALB/c mice were injected with 100µl of emulsion in both the dorsal proximal scruff and base of tail (150µg of OVA per mouse). Control groups included non-immunized mice and immunized mice that are not subsequently challenged with OVA. One week after immunization, aggregated OVA was prepared by suspending in PBS at a concentration of 10mg/ml in a 15ml tube. Solution was heated in 80ºC water bath for 60 minutes. Mice were then challenged with 300μg of aggregated OVA, by injecting 30μl of solution into the left footpad of immunized mice. After an additional week, mice were re-challenged in the same manner. (Non-immunized mice were also challenged at this step.) 24 hours after the second challenge, mice were euthanized by CO_2 asphyxiation and cervical dislocation. Each footpad of the mice was measured using calipers for swelling and weighed for changes in mass. Additionally, spleens were taken and processed for in vitro studies as indicated.

2.15. Experimental Autoimmune Encephalomyelitis.

For induced EAE (**Fig. 7A-I**), either Hooke Reagent or Myelin Oligodendrocyte Glycoprotein (MOG) (CSBio) and Complete Freund's Adjuvant (CFA) (Difco) emulsion was prepared. CFA/MOG emulsion was prepared in a 1:1 v/v ratio for a final concentration of 1000μg MOG per ml PBS. C57/B6 mice (Taconic) received 100μl of emulsion subcutaneously in the dorsal proximal scruff and base of the tail. About 2 hours after immunization, mice were injected intraperitoneally with 100μl of 2ng/μl pertussis toxin. 24 hours later, mice were injected again with 100μl of 2ng/μl pertussis toxin. Mice were monitored for disease every day and treated with 25mg/kg HLCL65 or DMSO vehicle control as indicated. At indicated timepoints, mice were euthanized by injection with 20mg/ml ketamine/4mg/ml xylazine (120μl per 20g mouse) and perfused with phosphate-buffered saline (PBS). Spleens, brains and spinal cords were collected from representative mice and processed for *in vitro* studies as indicated. To isolate brain and spinal cord mononuclear cells, brains and spinal cords were processed through a 70μm strainer and separated by a 70%-30% isotonic percoll gradient.

For spontaneous EAE (**Fig. 7J-L**), three MBP TCR Tg mice that developed EAE spontaneously (scores=1.5-2) were euthanized by CO_2 asphyxiation and cervical dislocation. Splenocytes were isolated and activated with 2μg/ml MBPAc1-11 for 48 hours in the presence of PRMT5 inhibitors or vehicle control. Tbet, IL-17, and RORγt expression were analyzed by intracellular flow cytometry.

3. Results

3.1. PRMT5 protein is up-regulated upon memory T cell reactivation.

PRMT5 is over-expressed in several lymphoid malignancies, where it promotes uncontrolled cell growth and survival of transformed cells (35). However, its role in non-malignant memory T cell proliferative responses is unknown. After exposure to their cognate antigen, previously sensitized T cells activate a signaling cascade that enhances metabolic activity and drives maximum proliferation 2-3 days post activation. Subsequently, the proliferative rate of T cells gradually decreases, and cells that survive the contraction period return to a non-proliferative resting state 7 days after activation (21). In order to determine whether PRMT5 plays a role in this process, PRMT5 expression was analyzed by Western blotting at various time-points after Myelin Basic Protein Ac_{1-11} (MBP)-specific T cell receptor (TCR) transgenic mouse memory Th1 or Th2 cells (characterized in **Supplemental Fig. 1**) were restimulated with immobilized anti-CD3/CD28. Compared to resting memory T cells, PRMT5 was up-regulated 2.5 fold in Th1 cells and 2.4 fold in Th2 cells at the 48 hour timepoint, the peak of PRMT5 expression (**Fig. 1A, B**). PRMT5 was subsequently down-regulated at day four, reaching baseline levels by day seven. These results led us to hypothesize that PRMT5 promotes proliferation during the normal cycle of T cell activation.

3.2. Selective PRMT5 inhibition blunts TCR-mediated memory T cell expansion.

To determine if PRMT5 activity is required for memory T cell proliferation, resting memory Th1 and Th2 T cells were activated *in vitro* and the extent of T cell expansion was measured by tritiated (^{3}H) thymidine incorporation assay in the presence of the previously described PRMT5 inhibitor, Compound 5 (CMP5) (51), or DMSO vehicle control. CMP5 was designed to selectively and reversibly bind within the PRMT5 active site to prevent transfer of the methyl group from donor S-adenosyl methionine, SAM, to the arginine substrate-binding pocket. CMP5 selectively inhibits PRMT5-mediated symmetric dimethylation but not other PRMTs (51). Overall, these data indicate that CMP5 is a selective PRMT5 inhibitor. CMP5 treatment of mTh1 and mTh2 cells strongly inhibited T cell proliferation (**Fig. 1C, E**). A detailed analysis of apoptosis status via Annexin V / PI staining revealed that there were no significant differences in apoptotic or dead cells in cells treated with PRMT5 inhibitor (**Fig 1D, F**), indicating that the reduced proliferation could not be explained by cell death. Interestingly, we noticed a small but significant difference in Th1 vs. Th2 suppression with CMP5. Th1 cell proliferation was more sensitive to PRMT5 inhibitors than Th2 cell proliferation (Th1: 95.4% inhibition; Th2: 90.5% inhibition, t test, $p<0.005$). To further explore this phenomenon, we analyzed the inhibitory concentration $(IC)_{50}$ values to PRMT5 inhibitor CMP5 for both cell types. Indeed, we confirmed that CMP5 more potently inhibited Th1 cell proliferation ($IC_{50} = 3.7$ μM) than Th2 cell proliferation ($IC_{50} = 9.2$ μM) (**Fig 1G, Table 1**). To determine if this phenomenon was isolated or if it would replicate with CMP5 derivatives, we treated cells with a second-generation bioavailable PRMT5-selective inhibitor, HLCL65 (**Supplemental Fig. 2A, B**). HLCL65 selectively inhibited PRMT5-mediated symmetric dimethylation (**Supplemental Fig. 2C, D**). HLCL65 inhibited T cell proliferation more potently than CMP5, but also suppressed Th1 cells ($IC_{50} = 1.1$ μM) more effectively than Th2 cells ($IC_{50} = 4.0$ μM) (**Fig. 1H, Table 1**). Overall, these data indicate that PRMT5 promotes murine memory T cell expansion and that inflammatory memory Th1 cells are more sensitive to targeting with PRMT5 inhibitors than Th2 cells. To determine whether the proliferation or differentiation of newly activated naïve T cells was similarly dependent on PRMT5 activity, we treated freshly isolated naïve $CD4^+$ T cells with

PRMT5 inhibitors. Both CMP5 and HLCL65 suppressed T cell proliferation in a dose-dependent manner (**Supplemental Fig. 3A, B**). Interestingly, and reminiscent of Th2 cells behavior, naïve $CD4^+$ T cells were more resistant than memory Th1 cells to PRMT5 inhibitors (**Supplemental Fig. 3A, B)**. We also observed decreased IFN-γ in supernatants from naive T cell cultures differentiated with CMP5 and HLCL65 in the absence of exogenous polarizing signals (**Supplemental Fig. 3C,D**). Overall, these results show preferential suppressive effects of PRMT5 inhibitors on memory Th1 responses that drive inflammatory autoimmune diseases such as MS.

3.3. PRMT5 is essential for human T cell activation and expansion.

Targeting of pathogenic Th cell expansion may be beneficial as a therapy in human Th1 mediated autoimmune diseases. To determine whether PRMT5 plays a similar role in human T cells, we restimulated previously differentiated human memory Th1- and Th2-enriched cells from healthy donors (characterized in **Supplemental Fig. 4**) and analyzed PRMT5 expression by Western blot from 0-7 days. We found that, similar to mouse T cells, PRMT5 was upregulated 2.1 fold in Th1 cells and 1.9 fold in Th2 cells by 48 hours post-activation **(Fig. 2A, B).** PRMT5 was then downregulated to resting levels by 7 days post-activation. Importantly, PRMT5 was also essential for the expansion of human T cells. The PRMT5-selective inhibitor, CMP5, preferentially suppressed human Th1 over Th2 cell proliferation (Th1: 43% inhibition, Th2: 9% inhibition, $p < 0.05$), **(Fig. 2C, E**) but had minimal effects on cell death (**Fig. 2D, F**)**.** To further evaluate the increased sensitivity of Th1 over Th2 cells to PRMT5 inhibition, we calculated the IC_{50} of human T cells when treated with CMP5 (Th1 IC_{50} = 26.9 μM vs Th2 IC_{50} = 31.6 μM) and HLCL65 (Th1 IC_{50} = 5.7 μM vs Th2 IC_{50} = 14.3 μM) **(Fig. 2G, H, Table 1).** To genetically validate a role for PRMT5 in proliferation, we knocked down PRMT5 expression via shRNA lentiviral transduction in human Th1 cells. PRMT5 shRNA partially reduced PRMT5 protein levels (45%) but not other PRMTs (1 and 7) and significantly decreased Th1 cell proliferation **(Fig. 3A).** Although significant, the mild suppression of proliferation could be explained by the low lentiviral transduction efficiency expected in primary T cells, coupled to the proliferative advantage of untransduced, i.e. PRMT5-sufficient, cells. To increase efficiency, we used the Neon Transfection System, which provided 70-90% transfection efficiency in our primary human Th1/2 cell lines (**Figure 3B**). Electroporation with either of three PRMT5-specific siRNAs efficiently suppressed human Th1 and Th2 cell proliferation to a degree that correlated with PRMT5 knockdown **(Fig. 3C-D).** These results validate a role for PRMT5 in T cell proliferative responses. Interestingly, we observed that PRMT5 siRNA transfection was accompanied by PRMT1 protein suppression, particularly in Th2 cells **(Fig. 3C-D)** cells. Since the three siRNAs target different areas in PRMT5 and all of them were confirmed to lack complementarity with PRMT1, it is unlikely that this is a direct effect of the siRNAs on PRMT1 but rather an indirect effect via PRMT5. Further studies should aim to elucidate the significance of this finding. Overall, these data indicate that PRMT5 is functionally conserved in both mouse and human T cells and plays a critical role in memory Th cell reactivation and expansion.

3.4. PRMT5 expression is dependent upon TCR-induced NF-κB signaling.

The NF-κB pathway has been associated with PRMT5 in hematologic malignancies (56) but the pathways involved in PRMT5 expression in T cells are unknown. T cell reactivation activates several signaling pathways, including the NF-κB pathway, leading to IL-2 production and proliferation. NF-κB transcription factors are kept inactive in the cytoplasm through binding to the inhibitory Iκ-B subunits. Upon T cell activation, the Iκ-B subunit is phosphorylated by IKKα and proteasomally degraded, allowing nuclear translocation of NF-κB and activation of transcription (57). To test whether NF-κB played a role in the up-regulation of PRMT5 expression after TCR/CD28 costimulation, we treated human Th cells with the IKK-α inhibitor Bay11-7082 (henceforth referred to as Bay11) during the first 8 hours of activation. After 48 hours of TCR/CD28 stimulation, we observed a decrease in PRMT5 protein levels in healthy human donor Th1 cells treated with Bay11 **(Fig. 4A).** In contrast, PRMT5 expression in Th2 cells was less dependent on NF-κB signaling than Th1 cells, as evidenced by stable levels of PRMT5 expression treated with Bay11 **(Fig. 4B)**. There were no differences in cell death with Bay11 treatment (**Fig. 4C, D),** indicating that the changes in protein expression observed could not be explained by cell death**.** As expected (58), NF-κB inhibition also resulted in a 65% reduction of downstream cytokine IL-2 levels in Th1 cells **(Fig. 4E).** These data are consistent with NF-κB signaling promoting PRMT5 expression and IL-2 secretion during TCR-mediated activation of Th1 and Th2 cells.

3.5. PRMT5 inhibition suppresses IL-2 secretion and IL-2 restoration rescues T cell expansion.

TCR mediated activation of the NF-κB pathway promotes IL-2, an important pro-proliferative T cell cytokine. We observed reduced IL-2 with Bay11-mediated suppression of PRMT5, and PRMT5 has been linked to IL-2 production in Jurkat cancer T cells (59). Therefore, we explored whether PRMT5 inhibition affected IL-2 secretion in reactivated mouse or human Th1 and Th2 mouse memory T cells. Vehicle treated mouse (**Fig. 5A**) and human (**Fig. 5B**) Th1 cells secreted high levels of IL-2 24 and 48 hours post-activation. In contrast, and as previously described in Th2 cells, (60), no IL-2 was detected in Th2 cells supernatants (data not shown). PRMT5 inhibition resulted in a reduction in IL-2 secretion that ranged from 50-75% for mouse Th1 cells and 30-80% for human Th1 cells (**Fig. 5A-B)**. These data suggested that loss of IL-2 secretion may contribute to the inhibition of proliferation observed with PRMT5 inhibition in Th1 cells. To test if the blunted T cell proliferation observed after PRMT5 inhibition could be rescued with IL-2 supplementation, memory Th1 cells were activated with anti-CD3/CD28 in the presence or absence of PRMT5 inhibitor and with increasing amounts of exogenous IL-2. Doses from 1 to 20 ng/ml were chosen since it was calculated that at least 10 ng/ml would be needed to restore the supernatant IL-2 levels observed in the vehicle Th1 condition (as in **Fig 5A**). T cell proliferation was evaluated through tritiated thymidine incorporation assay. Treatment with 25μM CMP5 inhibited mouse Th1 cell proliferation by 91% (t test $p<0.001$) (**Fig 5C**). As expected, addition of IL-2 enhanced proliferation in the vehicle condition, reaching a peak at 5 ng/ml. Addition of IL-2 in the presence of PRMT5 inhibitor increased proliferation in a dose-dependent manner, reaching 100% of the control values at 10 ng/ml **(Fig 5C).** Similarly, treatment with 25μM CMP5 suppressed human Th1 cell proliferation by 50%, and addition of exogenous IL-2 rescued proliferation (**Fig. 5D**). The recovery of Th1 T cell proliferation with exogenous IL-2 indicates that IL-2 pathways are active downstream of IL-2R and supports the notion that inhibition of IL-2 secretion by PRMT5 inhibitors contributes to the observed reduction in Th1 T cell proliferation. However additional mechanisms may also play a role in PRMT5 inhibitor-mediated suppression of proliferation, particularly in Th2 cells.

3.6. PRMT5 inhibition suppresses *in vivo* OVA-induced, delayed-type hypersensitivity inflammatory responses.

The effectiveness of PRMT5 inhibitors at suppressing inflammatory memory T cell responses suggested they may be beneficial in inflammatory or autoimmune disease. To test this, we used the ovalbumin (OVA)-induced delayed type hypersensitivity (DTH) mouse model and HLCL65, a more potent and bioavailable derivative of CMP5 (**Fig.1H, 2H, Supplemental Fig. 2**). First, we analyzed PRMT5 expression in the spleen after ovalbumin (OVA) immunization with Complete Freund's Adjuvant (CFA). We observed that 10 days post immunization, PRMT5 expression was significantly upregulated in the spleen (**Fig. 6A**), suggesting that PRMT5 expression is relevant to *in vivo* DTH immune responses. In the DTH model (outlined in **Fig. 6B**), ovalbumin (OVA) immunization with Complete Freund's Adjuvant (CFA) induces OVA-specific T cell response that causes footpad inflammation in mice upon subsequent exposure to adjuvant-free OVA and memory $CD4^+$ T cell expansion. HLCL65 treatment during the re-challenge period reduced footpad swelling by 40% ($p < 0.05$), a measure of inflammation (**Fig. 6C**). In addition, compared to vehicle, HLCL65 treatment reduced OVA-specific T cell proliferation by 36% (**Fig. 6D**) and IFN-γ production by 70% **(Fig. 6E).** These data indicate that our novel PRMT5 inhibitor HLCL65 suppresses T cell mediated responses and inflammation *in vivo.*

3.7. Prophylactic or therapeutic treatment with HLCL65 ameliorates Experimental Autoimmune Encephalomyelitis (EAE).

The ability of PRMT5 inhibitors to suppress *in vivo* inflammatory T cell responses could be beneficial in the autoimmune disease MS. We saw that PRMT5 was up-regulated in the spleen at

5 and 10 days after immunization with CFA/MOG (**Fig. 7A**), suggesting that PRMT5 plays an important role in the immune response against myelin antigens *in vivo*. In the myelin oligodendrocyte glycoprotein (MOG)-induced murine EAE model, T cell responses against this myelin antigen result in ascending paralysis. We first tested whether short-term prophylactic HLCL65 treatment (5 days 25mg/kg every other day starting at immunization) could prevent EAE. Indeed, HLCL65-treatment resulted in delayed disease onset (16.9 days for HLCL65-treated mice vs. 13.4 days for vehicle treated mice) and a 33% reduction in disease incidence, compared to vehicle-treated mice **(Table 2).** Importantly, HLCL65-treated mice presented reduced EAE disease burden, as measured by Area Under the Curve (AUC), compared to vehicle control (AUC HLCL65 vs. vehicle: 8.2 vs. 2.1, $p = 0.016$) **(Fig. 7B, Table 2).** These clinical effects were associated with reduced MOG-specific T cell proliferative responses (**Fig. 7C**), reduced CNS IL-17 production (**Fig. 7D**), and suppressed *Tbet* mRNA expression in the CNS (**Fig. 7E)**. With these promising results, we tested HLCL65 during a therapeutically relevant window for MS patients, i.e., after clinical signs had developed. HLCL65 treatment, beginning at 14 days post-immunization (average score at treatment initiation = 2.7 out of 5), suppressed existing EAE clinical signs as measured by the total disease burden (AUC HLCL65 vs. vehicle: 19.1 ± 1.6 vs 27.31 ± 3.1, **Fig. 7F, Table 3**). This disease suppression correlated with a reduction in MOG-specific T cell proliferation of HLCL65-treated mice (**Fig. 7G**). Additionally, inflammatory Th1 and Th17 responses were diminished in HLCL65-treated mice (**Fig. 7H, I**). These data further support that PRMT5 activity may be essential for T cell function, and our novel PRMT5-selective inhibitors effectively suppress T cell-mediated inflammation. Next, to test whether PRMT5 inhibitors could suppress preformed encephalitogenic Th17 cells, splenocytes from MBP TCR Tg that had spontaneously developed EAE (average score = 1.7)

were activated with antigen in the presence or absence of CMP5 and HLCL65. CMP5 treatment significantly suppressed IL-17$^+$RORγt$^+$ (**Fig. 7J**) Th17 cells and, particularly, a pathogenic T-bet$^+$RORγt$^+$ population(61) (**Fig. 7K**) in a dose-dependent manner. A similar dose-dependent decrease in pathogenic T-bet$^+$IL-17$^+$ Th17 cell population(62) was apparent, but did not reach statitistical significance (**Fig. 7J-L)**. Similar results were observed with HLCL65 treatment (data not shown). Taken together, these results indicate that PRMT5 promotes pathogenic Th1 and Th17 cell responses that promote inflammation and autoimmunity.

4. Discussion

Memory T cell reactivation after antigen exposure rapidly induces T cell proliferation and effector function. This process can be beneficial, as in vaccination immunity, or deleterious, as in perpetuation of pathogenic responses in autoimmunity. Here, we show by expression knockdown and pharmacologic means that PRMT5, a methyltransferase that catalyzes symmetric dimethylation of arginine residues in histones and other proteins, promotes the activation and expansion of memory Th lymphocytes following antigen re-exposure.

The first indications of a key role for arginine methylation in lymphocyte activation originated from conditions and treatments that inhibit all SAM-dependent methylation reactions (25, 26). PRMTs have been proposed to mediate some of these effects (29), but the role of individual PRMTs in these processes remained unresolved. We found that antigen re-exposure in memory T cells up-regulates PRMT5 expression as T cells proliferate and expand, followed by a contraction phase in which PRMT5 expression is progressively lost. The temporal link between PRMT5 expression and proliferation, together with the observed inhibition of proliferation upon selective PRMT5 inhibition, indicates that PRMT5 activity is necessary for TCR engagement-induced memory T cell expansion. Th2 cell expansion was less dependent on PRMT5 activity than that of Th1 cells. This difference was reproduced in both mouse and human Th cells, indicating that this is a conserved difference that may impact human disease. However, differential sensitivity to PRMT5 inhibition did not appear to stem from differences in PRMT5 expression, which was equivalent in Th1 and Th2 cells. It is possible that PRMT5 activity is lower in Th2 than Th1 cells due to expression of type I methyltransferases, which compete for substrates with PRMT5 (63). This difference offers the intriguing possibility that targeting

PRMT5 may modulate the Th1/Th2 balance defect observed in autoimmune/inflammatory diseaseas such as Multiple Sclerosis (12, 13).

The exact chain of events that leads to PRMT5 up-regulation in T cells is unclear. A link between the NF-kB pathway leading to activation of the repressive p65/HDAC/Sp1 complex and loss of PRMT5 targeting miRNA has been reported in mantle cell lymphoma (64). We had also previously found that NF-κB inhibition suppresses PRMT5 expression in EBV-transformed cells (51). Since TCR engagement activates the NF-κB pathway in T cells, a similar mechanism may regulate PRMT5 expression in T cells. Indeed, blocking NF-κB signaling attenuated, but did not completely erase, PRMT5 expression in human Th1, but not Th2, cells. This indicates that while NF-κB is an important driver of PRMT5 expression in Th1 cells, other TCR-induced pathways play a more significant role in regulating PRMT5 expression, especially in Th2 cells. TCR signaling cascades include the NFAT, Erk1/2, p38 and JNK MAPK. Interestingly, inhibitors of the p38 and JNK-MAPK, but not ERK1/2, pathway have been shown to inhibit hypoxia-induced up-regulation of PRMT5 in lung epithelial cells (65). While future studies will be required to clarify the extent to which these pathways affect PRMT5 up-regulation in T cells, NF-κB appears to play a major role in TCR-induced PRMT5 expression in human Th1, but not Th2, cells. Additionally, several studies have shown that PRMT5 activates NF-κB signaling through arginine methylation of p65 (56, 66-68), suggesting that the NF-κB-PRMT5 signaling axis could involve a positive feedback loop. Additional studies are required to validate this feedback loop and evaluate its role in T cells.

Several pathways downstream of TCR activation converge on activation of the IL-2 promoter to induce T cell proliferation (18, 19, 69). Here, we found that IL-2 secretion is dependent on PRMT5 activity and that exogenous IL-2 addition to PRMT5 inhibitor-treated cells restored proliferation in Th1 cells. A role for PRMT5 in IL-2 production is consistent with the observations by Richard *et al* that PRMT5 siRNA suppresses IL-2 secretion in the Jurkat cancer T cell line (59). This effect is thought to be mediated by PRMT5-catalyzed arginine methylation on histones. In support of this hypothesis, symmetrically dimethylated proteins associate to the IL-2 promoter after T cell activation. In contrast, PRMT5 did not directly associate with the IL-2 promoter. These data are consistent with PRMT5 indirectly regulating IL-2 expression, via SDM of target proteins. Although the specific proteins that are methylated and bind to the IL-2 promoter remain to be defined, two proteins that form an IL-2 promoter-binding complex, namely NF-45 and NF-90, have been proposed as candidate targets(59). Another candidate is the TCR signaling protein Vav-1, whose SDM has been reported to promote IL-2 expression (70). Overall, our data point to IL-2 as one of the mechanisms by which PRMT5 regulates proliferation in Th1 cells. However, since we observe only a 60% reduction in IL-2 production yet T cell proliferation is reduced by 90-95% when treated with CMP5, it is likely that PRMT5 regulates proliferation by several mechanisms. As Th2 cells do not secrete large amounts of IL-2, further studies are required to determine the mechanism by which PRMT5 promotes Th2 cell proliferation.

Memory T cell responses play a critical role in chronic T cell-mediated diseases such as autoimmunity and allergy (71, 72). For example, increased memory T cells have been found in MS patients with active disease and further increase during disease flare (4), while the memory to naïve T cell ratio diminishes in patients responding to therapy (73). Importantly, inhibition of methyltransferases successfully suppresses T cell activation and established clinical EAE and other inflammatory/autoimmune diseases (25-28) but the lack of selectivity has so far prevented the development of these treatments as a therapy. Our data indicates that selective PRMT5 inhibition reproduces the suppression of memory T cell expansion observed with pan-methyltransferase inhibitors and may be similarly effective in autoimmunity. Indeed, *in vivo* treatment with PRMT5 inhibitors was able to suppress two models of inflammatory/autoimmune disease, i.e., DTH footpad inflammation and EAE Central Nervous System (CNS) inflammation. PRMT5 inhibitors were effective at suppressing clinically established EAE disease. While a contribution of PRMT5 inhibition in non-T cells, i.e. CNS cells or antigen-presenting cells (APCs), to EAE suppression cannot be ruled out, our data is consistent with T cell being a major target. Effects on APCs could result on reduced TcR engagement and T cell responses. However, *in vitro* experiments showed similar suppressive effects when T cells are activated by anti-CD3/CD28 (**Fig. 1E**) or antigen-loaded APCs (**Fig. 1C**). In addition, EAE HLCL65 treatment suppressed previously generated T cell responses that are less dependent on APC costimulation. The similarity in suppression of proliferation and inflammatory cytokines from *in vitro* and in *vivo* DTH/EAE studies is also consistent with T cells being a major target. To investigate relevance to human disease, we analyzed genome-wide association studies from the International Multiple Sclerosis Genetics Consortium and the Wellcome Trust Case Control Consortium. Interestingly, rs4410871 was identified as a high frequency SNP in the *MYC* locus in multiple sclerosis patients (74). MYC has been shown to be upregulated after T cell activation (75) and also, to promote PRMT5 expression (37, 38). Taken together, these data suggest that PRMT5 could play a significant role in human disease.

In summary, this is the first report of the role of PRMT5 expression in *in vitro* and *in vivo* non-malignant T cell responses. Our work identifies PRMT5 as an epigenetic modifier enzyme that promotes memory Th cell expansion. Memory T cell expansion of inflammatory Th1 and, to a lesser extent, Th2 cells was dependent on PRMT5 activity. Finally, PRMT5 inhibitors suppressed T cell mediated inflammatory and autoimmune disease, suggesting that PRMT5 may be a promising therapeutic target for autoimmune and other T cell mediated diseases.

Conflict of Interest

RAB and CL have a patent on PRMT5 inhibitors. The remaining authors declare no commercial or financial conflict of interest.

Acknowledgements

We would like to thank Chad Bennett, Erandi De Silva, Larry Schaaf and Bence Boelscewski at the Drug Development Institute team for their insightful discussions.

References

1. *http://www.who.int/mental_health/neurology/Atlas_MS_WEB.pdf*.
2. Frohman, E. M., M. K. Racke, and C. S. Raine. 2006. Multiple sclerosis--the plaque and its pathogenesis. *N Engl J Med* 354: 942–955.
3. Crucian, B., P. Dunne, H. Friedman, R. Ragsdale, S. Pross, and R. Widen. 1995. Alterations in peripheral blood mononuclear cell cytokine production in response to phytohemagglutinin in multiple sclerosis patients. *Clin. Diagn. Lab. Immunol.* 2: 766–769.
4. Okuda, Y., M. Okuda, B. R. Apatoff, and D. N. Posnett. 2005. The activation of memory CD4(+) T cells and CD8(+) T cells in patients with multiple sclerosis. *J. Neurol. Sci.* 235: 11–17.
5. Khoury, S. J., C. R. Guttmann, E. J. Orav, R. Kikinis, F. A. Jolesz, and H. L. Weiner. 2000. Changes in activated T cells in the blood correlate with disease activity in multiple sclerosis. *Arch Neurol* 57: 1183–1189.
6. Putheti, P., M. Morris, L. Stawiarz, N. Teleshova, P. Kivisäkk, M. Pashenkov, M. Kouwenhoven, M. K. Wiberg, L. Bronge, Y.-M. Huang, M. Söderström, J. Hillert, and H. Link. 2003. Multiple sclerosis: a study of chemokine receptors and regulatory T cells in relation to MRI variables. *Eur. J. Neurol.* 10: 529–535.
7. Jensen, J., A. R. Langkilde, C. Fenst, M. S. Nicolaisen, H. G. Roed, M. Christiansen, and F. Sellebjerg. 2004. CD4 T cell activation and disease activity at onset of multiple sclerosis. *J Neuroimmunol* 149: 202–209.
8. Scolozzi, R., A. Boccafogli, M. R. Tola, L. Vicentini, A. Camerani, D. Degani, E. Granieri, L. Caniatti, and E. Paolino. 1992. T-cell phenotypic profiles in the cerebrospinal fluid and peripheral blood of multiple sclerosis patients. *J. Neurol. Sci.* 108: 93–98.
9. Kebir, H., K. Kreymborg, I. Ifergan, A. Dodelet-Devillers, R. Cayrol, M. Bernard, F. Giuliani, N. Arbour, B. Becher, and A. Prat. 2007. Human TH17 lymphocytes promote blood-brain barrier disruption and central nervous system inflammation. *Nat Med* 13: 1173–1175.
10. Venken, K., N. Hellings, M. Thewissen, V. Somers, K. Hensen, J.-L. Rummens, R. Medaer, R. Hupperts, and P. Stinissen. 2008. Compromised CD4+ CD25(high) regulatory T-cell function in patients with relapsing-remitting multiple sclerosis is correlated with a reduced frequency of FOXP3-positive cells and reduced FOXP3 expression at the single-cell level. *Immunology* 123: 79–89.
11. Windhagen, A., D. E. Anderson, A. Carrizosa, K. Balashov, H. L. Weiner, and D. A. Hafler. 1998. Cytokine secretion of myelin basic protein reactive T cells in patients with multiple sclerosis. *J Neuroimmunol* 91: 1–9.
12. Guerau-de-Arellano, M., K. M. Smith, J. Godlewski, Y. Liu, R. Winger, S. E. Lawler, C. C. Whitacre, M. K. Racke, and A. E. Lovett-Racke. 2011. Micro-RNA dysregulation in multiple sclerosis favours pro-inflammatory T-cell-mediated autoimmunity. *Brain* 134: 3578–3589.
13. Couturier, N., F. Bucciarelli, R. N. Nurtdinov, M. Debouverie, C. Lebrun-Frenay, G. Defer, T. Moreau, C. Confavreux, S. Vukusic, I. Cournu-Rebeix, R. H. Goertsches, U. K. Zettl, M. Comabella, X. Montalban, P. Rieckmann, F. Weber, B. Müller-Myhsok, G. Edan, B. Fontaine, L. T. Mars, A. Saoudi, J. R. Oksenberg, M. Clanet, R. S. Liblau, and D. Brassat. 2011. Tyrosine kinase 2 variant influences T lymphocyte polarization and multiple sclerosis susceptibility. *Brain* 134: 693–703.
14. Raddassi, K., S. C. Kent, J. Yang, K. Bourcier, E. M. Bradshaw, V. Seyfert-Margolis, G. T. Nepom, W. W. Kwok, and D. A. Hafler. 2011. Increased Frequencies of Myelin Oligodendrocyte Glycoprotein/MHC Class II-Binding CD4 Cells in Patients with Multiple Sclerosis. *The Journal of Immunology* 187: 1039–1046.

15. Lovett-Racke, A. E., J. L. Trotter, J. Lauber, P. J. Perrin, C. H. June, and M. K. Racke. 1998. Decreased dependence of myelin basic protein-reactive T cells on CD28-mediated costimulation in multiple sclerosis patients. A marker of activated/memory T cells. *J Clin Invest* 101: 725–730.
16. Cao, Y., B. A. Goods, K. Raddassi, G. T. Nepom, W. W. Kwok, J. C. Love, and D. A. Hafler. 2015. Functional inflammatory profiles distinguish myelin-reactive T cells from patients with multiple sclerosis. *Science Translational Medicine* 7: 287ra74–287ra74.
17. Nakayama, T., and M. Yamashita. 2010. The TCR-mediated signaling pathways that control the direction of helper T cell differentiation. *Semin Immunol* 22: 303–309.
18. Jain, J., C. Loh, and A. Rao. 1995. Transcriptional regulation of the IL-2 gene. *Curr Opin Immunol* 7: 333–342.
19. Guy, C. S., K. M. Vignali, J. Temirov, M. L. Bettini, A. E. Overacre, M. Smeltzer, H. Zhang, J. B. Huppa, Y.-H. Tsai, C. Lobry, J. Xie, P. J. Dempsey, H. C. Crawford, I. Aifantis, M. M. Davis, and D. A. A. Vignali. 2013. Distinct TCR signaling pathways drive proliferation and cytokine production in T cells. *Nat Immunol* 14: 262–270.
20. Huang, W., and A. August. 2015. The signaling symphony: T cell receptor tunes cytokine-mediated T cell differentiation. *J. Leukoc. Biol.* 97: 477–485.
21. Corradin, G., H. M. Etlinger, and J. M. Chiller. 1977. Lymphocyte specificity to protein antigens. I. Characterization of the antigen-induced in vitro T cell-dependent proliferative response with lymph node cells from primed mice. *The Journal of Immunology* 119: 1048–1053.
22. Cassani, B., M. Mirolo, F. Cattaneo, U. Benninghoff, M. Hershfield, F. Carlucci, A. Tabucchi, C. Bordignon, M. G. Roncarolo, and A. Aiuti. 2008. Altered intracellular and extracellular signaling leads to impaired T-cell functions in ADA-SCID patients. *Blood* 111: 4209–4219.
23. Blaese, R. M., K. W. Culver, A. D. Miller, C. S. Carter, T. Fleisher, M. Clerici, G. Shearer, L. Chang, Y. Chiang, P. Tolstoshev, J. J. Greenblatt, S. A. Rosenberg, H. Klein, M. Berger, C. A. Mullen, W. J. Ramsey, L. Muul, R. A. Morgan, and W. F. Anderson. 1995. T lymphocyte-directed gene therapy for ADA- SCID: initial trial results after 4 years. *Science* 270: 475–480.
24. German, D. C., C. A. Bloch, and N. M. Kredich. 1983. Measurements of S-adenosylmethionine and L-homocysteine metabolism in cultured human lymphoid cells. *J Biol Chem* 258: 10997–11003.
25. Yang, M.-L., A. J. P. Gee, R. J. Gee, C. I. Zurita-Lopez, S. Khare, S. G. Clarke, and M. J. Mamula. 2013. Lupus autoimmunity altered by cellular methylation metabolism. *Autoimmunity* 46: 21–31.
26. Saso, Y., E. M. Conner, B. R. Teegarden, and C. S. Yuan. 2001. S-Adenosyl-L-homocysteine hydrolase inhibitor mediates immunosuppressive effects in vivo: suppression of delayed type hypersensitivity ear swelling and peptidoglycan polysaccharide-induced arthritis. *J. Pharmacol. Exp. Ther.* 296: 106–112.
27. Moreno, B., H. Hevia, M. Santamaria, J. Sepulcre, J. Muñoz, E. R. García-Trevijano, C. Berasain, F. J. Corrales, M. A. Avila, and P. Villoslada. 2006. Methylthioadenosine reverses brain autoimmune disease. *Ann. Neurol.* 60: 323–334.
28. Moreno, B., B. Fernandez-Diez, A. Di Penta, and P. Villoslada. 2010. Preclinical studies of methylthioadenosine for the treatment of multiple sclerosis. *Mult Scler* 16: 1102–1108.
29. Parry, R. V., and S. G. Ward. 2010. Protein arginine methylation: a new handle on T lymphocytes? *Trends Immunol* 31: 164–169.
30. Henrich, F. C., K. Singer, K. Poller, L. Bernhardt, C. D. Strobl, K. Limm, A. P. Ritter, E. Gottfried, S. Völkl, B. Jacobs, K. Peter, D. Mougiakakos, K. Dettmer, P. J. Oefner, A.-K.

Bosserhoff, M. P. Kreutz, M. Aigner, and A. Mackensen. 2016. Suppressive effects of tumor cell-derived 5′-deoxy-5′-methylthioadenosine on human T cells. *OncoImmunology* 5: e1184802.

31. Gary, J. D., and S. Clarke. 1998. RNA and protein interactions modulated by protein arginine methylation. *Prog. Nucleic Acid Res. Mol. Biol.* 61: 65–131.

32. Yang, Y., A. Hadjikyriacou, Z. Xia, S. Gayatri, D. Kim, C. Zurita-Lopez, R. Kelly, A. Guo, W. Li, S. G. Clarke, and M. T. Bedford. 2015. PRMT9 is a type II methyltransferase that methylates the splicing factor SAP145. *Nat Commun* 6: 6428.

33. Zurita-Lopez, C. I., T. Sandberg, R. Kelly, and S. G. Clarke. 2012. Human protein arginine methyltransferase 7 (PRMT7) is a type III enzyme forming ω-NG-monomethylated arginine residues. *J Biol Chem* 287: 7859–7870.

34. Bedford, M. T. 2007. Arginine methylation at a glance. *J. Cell. Sci.* 120: 4243–4246.

35. Stopa, N., J. E. Krebs, and D. Shechter. 2015. The PRMT5 arginine methyltransferase: many roles in development, cancer and beyond. *Cell. Mol. Life Sci.* 72: 2041–2059.

36. Karkhanis, V., Y.-J. Hu, R. A. Baiocchi, A. N. Imbalzano, and S. Sif. 2011. Versatility of PRMT5-induced methylation in growth control and development. *Trends Biochem. Sci.* 36: 633–641.

37. Koh, C. M., M. Bezzi, D. H. P. Low, W. X. Ang, S. X. Teo, F. P. H. Gay, M. Al-Haddawi, S. Y. Tan, M. Osato, A. Sabò, B. Amati, K. B. Wee, and E. Guccione. 2015. MYC regulates the core pre-mRNA splicing machinery as an essential step in lymphomagenesis. *Nature* 523: 96–100.

38. Li, Y., N. Chitnis, H. Nakagawa, Y. Kita, S. Natsugoe, Y. Yang, Z. Li, M. Wasik, A. J. P. Klein-Szanto, A. K. Rustgi, and J. A. Diehl. 2015. PRMT5 Is Required for Lymphomagenesis Triggered by Multiple Oncogenic Drivers. *Cancer Discovery* 5: 288–303.

39. Pal, S., R. A. Baiocchi, J. C. Byrd, M. R. Grever, S. T. Jacob, and S. Sif. 2007. Low levels of miR-92b/96 induce PRMT5 translation and H3R8/H4R3 methylation in mantle cell lymphoma. *EMBO J.* 26: 3558–3569.

40. Wang, L., S. Pal, and S. Sif. 2008. Protein arginine methyltransferase 5 suppresses the transcription of the RB family of tumor suppressors in leukemia and lymphoma cells. *Mol Cell Biol* 28: 6262–6277.

41. Chung, J., V. Karkhanis, S. Tae, F. Yan, P. Smith, L. W. Ayers, C. Agostinelli, S. Pileri, G. V. Denis, R. A. Baiocchi, and S. Sif. 2013. Protein arginine methyltransferase 5 (PRMT5) inhibition induces lymphoma cell death through reactivation of the retinoblastoma tumor suppressor pathway and polycomb repressor complex 2 (PRC2) silencing. *J Biol Chem* 288: 35534–35547.

42. Shilo, K., X. Wu, S. Sharma, M. Welliver, W. Duan, M. Villalona-Calero, J. Fukuoka, S. Sif, R. Baiocchi, C. L. Hitchcock, W. Zhao, and G. A. Otterson. 2013. Cellular localization of protein arginine methyltransferase-5 correlates with grade of lung tumors. *Diagn Pathol* 8: 201.

43. Yan, F., L. Alinari, M. E. Lustberg, L. K. Martin, H. M. Cordero-Nieves, Y. Banasavadi-Siddegowda, S. Virk, J. Barnholtz-Sloan, E. H. Bell, J. Wojton, N. K. Jacob, A. Chakravarti, M. O. Nowicki, X. Wu, R. Lapalombella, J. Datta, B. Yu, K. Gordon, A. Haseley, J. T. Patton, P. L. Smith, J. Ryu, X. Zhang, X. Mo, G. Marcucci, G. Nuovo, C.-H. Kwon, J. C. Byrd, E. A. Chiocca, C. Li, S. Sif, S. Jacob, S. Lawler, B. Kaur, and R. A. Baiocchi. 2014. Genetic validation of the protein arginine methyltransferase PRMT5 as a candidate therapeutic target in glioblastoma. *Cancer Res*.

44. Han, X., R. Li, W. Zhang, X. Yang, C. G. Wheeler, G. K. Friedman, P. Province, Q. Ding, Z. You, H. M. Fathallah-Shaykh, G. Y. Gillespie, X. Zhao, P. H. King, and L. B. Nabors. 2014.

Expression of PRMT5 correlates with malignant grade in gliomas and plays a pivotal role in tumor growth in vitro. *J Neurooncol* 118: 61–72.

45. Powers, M. A., M. M. Fay, R. E. Factor, A. L. Welm, and K. S. Ullman. 2011. Protein Arginine Methyltransferase 5 Accelerates Tumor Growth by Arginine Methylation of the Tumor Suppressor Programmed Cell Death 4. *Cancer Res* 71: 5579–5587.

46. Gu, Z., S. Gao, F. Zhang, Z. Wang, W. Ma, R. E. Davis, and Z. Wang. 2012. Protein arginine methyltransferase 5 is essential for growth of lung cancer cells. *Biochemical Journal* 446: 235–241.

47. Bao, X., S. Zhao, T. Liu, Y. Liu, Y. Liu, and X. Yang. 2013. Overexpression of PRMT5 Promotes Tumor Cell Growth and Is Associated with Poor Disease Prognosis in Epithelial Ovarian Cancer. *J Histochem Cytochem* 61: 206–217.

48. Kim, J.-M., H.-Y. Sohn, S. Y. Yoon, J.-H. Oh, J. O. Yang, J. H. Kim, K. S. Song, S.-M. Rho, H. S. Yoo, Y. S. Kim, J.-G. Kim, and N.-S. Kim. 2005. Identification of Gastric Cancer–Related Genes Using a cDNA Microarray Containing Novel Expressed Sequence Tags Expressed in Gastric Cancer Cells. *Clin Cancer Res* 11: 473–482.

49. Cho, E. C., S. Zheng, S. Munro, G. Liu, S. M. Carr, J. Moehlenbrink, Y. C. Lu, L. Stimson, O. Khan, R. Konietzny, J. McGouran, A. S. Coutts, B. Kessler, D. J. Kerr, and N. B. La Thangue. 2012. Arginine methylation controls growth regulation by E2F-1. *EMBO J.* 31: 1785–1797.

50. Panfil, A., J. Al-Saleem, C. Howard, J. Mates, J. Kwiek, R. Baiocchi, and P. Green. 2015. PRMT5 Is Upregulated in HTLV-1-Mediated T-Cell Transformation and Selective Inhibition Alters Viral Gene Expression and Infected Cell Survival. *Viruses 2016, Vol. 8, Page 7* 8: 7.

51. Alinari, L., K. V. Mahasenan, F. Yan, V. Karkhanis, J.-H. Chung, E. M. Smith, C. Quinion, P. L. Smith, L. Kim, J. T. Patton, R. Lapalombella, B. Yu, Y. Wu, S. Roy, A. De Leo, S. Pileri, C. Agostinelli, L. Ayers, J. E. Bradner, S. Chen-Kiang, O. Elemento, T. Motiwala, S. Majumder, J. C. Byrd, S. Jacob, S. Sif, C. Li, and R. A. Baiocchi. 2015. Selective inhibition of protein arginine methyltransferase 5 blocks initiation and maintenance of B-cell transformation. *Blood.*

52. Chan-Penebre, E., K. G. Kuplast, C. R. Majer, P. A. Boriack-Sjodin, T. J. Wigle, L. D. Johnston, N. Rioux, M. J. Munchhof, L. Jin, S. L. Jacques, K. A. West, T. Lingaraj, K. Stickland, S. A. Ribich, A. Raimondi, M. P. Scott, N. J. Waters, R. M. Pollock, J. J. Smith, O. Barbash, M. Pappalardi, T. F. Ho, K. Nurse, K. P. Oza, K. T. Gallagher, R. Kruger, M. P. Moyer, R. A. Copeland, R. Chesworth, and K. W. Duncan. 2015. A selective inhibitor of PRMT5 with in vivo and in vitro potency in MCL models. *Nat. Chem. Biol.* 11: 432–437.

53. Goverman, J., A. Woods, L. Larson, L. P. Weiner, L. Hood, and D. M. Zaller. 1993. Transgenic mice that express a myelin basic protein-specific T cell receptor develop spontaneous autoimmunity. *Cell* 72: 551–560.

54. Pal, S., S. N. Vishwanath, H. Erdjument-Bromage, P. Tempst, and S. Sif. 2004. Human SWI/SNF-associated PRMT5 methylates histone H3 arginine 8 and negatively regulates expression of ST7 and NM23 tumor suppressor genes. *Mol Cell Biol* 24: 9630–9645.

55. Zhao, X., S. Chen-Kiang, S. Shetty, M. Di Liberto, J. Bodo, L. Durkin, K. Eng, O. Elemento, M. R. Smith, and E. D. Hsi. 2015. CCMCL1: a new model of aggressive mantle cell lymphoma. *Blood* 125: 2730–2732.

56. Tanaka, H., Y. Hoshikawa, T. Oh-hara, S. Koike, M. Naito, T. Noda, H. Arai, T. Tsuruo, and N. Fujita. 2009. PRMT5, a novel TRAIL receptor-binding protein, inhibits TRAIL-induced apoptosis via nuclear factor-kappaB activation. *Mol. Cancer Res.* 7: 557–569.

57. Nomura, Kawai, K. Nakanishi, and S. Akira. 2000. NF-κB activation through IKK-i-

dependent I-TRAF/TANK phosphorylation. *Genes Cells* 5: 191–202.

58. Sriskantharajah, S., M. P. Belich, S. Papoutsopoulou, J. Janzen, V. Tybulewicz, B. Seddon, and S. C. Ley. 2009. Proteolysis of NF-kappaB1 p105 is essential for T cell antigen receptor-induced proliferation. *Nat Immunol* 10: 38–47.

59. Richard, S., M. Morel, and P. Cléroux. 2005. Arginine methylation regulates IL-2 gene expression: a role for protein arginine methyltransferase 5 (PRMT5). *Biochem. J.* 388: 379–386.

60. Mosmann, T. R., and R. L. Coffman. 1989. TH1 and TH2 cells: different patterns of lymphokine secretion lead to different functional properties. *Annu Rev Immunol* 7: 145–173.

61. Ghoreschi, K., A. Laurence, X.-P. Yang, C. M. Tato, M. J. McGeachy, J. E. Konkel, H. L. Ramos, L. Wei, T. S. Davidson, N. Bouladoux, J. R. Grainger, Q. Chen, Y. Kanno, W. T. Watford, H.-W. Sun, G. Eberl, E. M. Shevach, Y. Belkaid, D. J. Cua, W. Chen, and J. J. O'Shea. 2010. Generation of pathogenic T(H)17 cells in the absence of TGF-β signalling. *Nature* 467: 967–971.

62. Yang, Y., J. Weiner, Y. Liu, A. J. Smith, D. J. Huss, R. Winger, H. Peng, P. D. Cravens, M. K. Racke, and A. E. Lovett-Racke. 2009. T-bet is essential for encephalitogenicity of both Th1 and Th17 cells. *J Exp Med* 206: 1549–1564.

63. Bonham, K., S. Hemmers, Y.-H. Lim, D. M. Hill, M. G. Finn, and K. A. Mowen. 2010. Effects of a novel arginine methyltransferase inhibitor on T-helper cell cytokine production. *FEBS J.* 277: 2096–2108.

64. Liu, S., L.-C. Wu, J. Pang, R. Santhanam, S. Schwind, Y.-Z. Wu, C. J. Hickey, J. Yu, H. Becker, K. Maharry, M. D. Radmacher, C. Li, S. P. Whitman, A. Mishra, N. Stauffer, A. M. Eiring, R. Briesewitz, R. A. Baiocchi, K. K. Chan, P. Paschka, M. A. Caligiuri, J. C. Byrd, C. M. Croce, C. D. Bloomfield, D. Perrotti, R. Garzon, and G. Marcucci. 2010. Sp1/NFkappaB/HDAC/miR-29b regulatory network in KIT-driven myeloid leukemia. *Cancer Cell* 17: 333–347.

65. Lim, S. K., Y. W. Jeong, D. I. Kim, M. J. Park, J. H. Choi, S. U. Kim, S. S. Kang, H. J. Han, and S. H. Park. 2013. Activation of PRMT1 and PRMT5 mediates hypoxia- and ischemia-induced apoptosis in human lung epithelial cells and the lung of miniature pigs: the role of p38 and JNK mitogen-activated protein kinases. *Biochem Biophys Res Commun* 440: 707–713.

66. Lu, T., and G. R. Stark. 2015. NF-κB: Regulation by Methylation. *Cancer Res* 75: 3692–3695.

67. Wei, H., B. Wang, M. Miyagi, Y. She, B. Gopalan, D.-B. Huang, G. Ghosh, G. R. Stark, and T. Lu. 2013. PRMT5 dimethylates R30 of the p65 subunit to activate NF-κB. *Proc Natl Acad Sci USA* 110: 13516–13521.

68. Harris, D. P., S. Bandyopadhyay, T. J. Maxwell, B. Willard, and P. E. Dicorleto. 2014. Tumor Necrosis Factor (TNF)-α Induction of CXCL10 in Endothelial Cells Requires Protein Arginine Methyltransferase 5 (PRMT5)-mediated Nuclear Factor (NF)-κB p65 Methylation. *J Biol Chem* 289: 15328–15339.

69. Kemp, M. L., L. Wille, C. L. Lewis, L. B. Nicholson, and D. A. Lauffenburger. 2007. Quantitative network signal combinations downstream of TCR activation can predict IL-2 production response. *The Journal of Immunology* 178: 4984–4992.

70. Blanchet, F., A. Cardona, F. A. Letimier, M. S. Hershfield, and O. Acuto. 2005. CD28 costimulatory signal induces protein arginine methylation in T cells. *J Exp Med* 202: 371–377.

71. Devarajan, P., and Z. Chen. 2013. Autoimmune effector memory T cells: the bad and the good. *Immunol. Res.* 57: 12–22.

72. Endo, Y., K. Hirahara, R. Yagi, D. J. Tumes, and T. Nakayama. 2014. Pathogenic memory

type Th2 cells in allergic inflammation. *Trends Immunol* 35: 69–78.

73. Blanco, Y., E. A. Moral, M. Costa, M. Gómez-Choco, J. F. Torres-Peraza, L. Alonso-Magdalena, J. Alberch, D. Jaraquemada, T. Arbizu, F. Graus, and A. Saiz. 2006. Effect of glatiramer acetate (Copaxone) on the immunophenotypic and cytokine profile and BDNF production in multiple sclerosis: a longitudinal study. *Neurosci. Lett.* 406: 270–275.

74. International Multiple Sclerosis Genetics Consortium, Wellcome Trust Case Control Consortium 2, S. Sawcer, G. Hellenthal, M. Pirinen, C. C. A. Spencer, N. A. Patsopoulos, L. Moutsianas, A. Dilthey, Z. Su, C. Freeman, S. E. Hunt, S. Edkins, E. Gray, D. R. Booth, S. C. Potter, A. Goris, G. Band, A. B. Oturai, A. Strange, J. Saarela, C. Bellenguez, B. Fontaine, M. Gillman, B. Hemmer, R. Gwilliam, F. Zipp, A. Jayakumar, R. Martin, S. Leslie, S. Hawkins, E. Giannoulatou, S. D'alfonso, H. Blackburn, F. M. Boneschi, J. Liddle, H. F. Harbo, M. L. Perez, A. Spurkland, M. J. Waller, M. P. Mycko, M. Ricketts, M. Comabella, N. Hammond, I. Kockum, O. T. McCann, M. Ban, P. Whittaker, A. Kemppinen, P. Weston, C. Hawkins, S. Widaa, J. Zajicek, S. Dronov, N. Robertson, S. J. Bumpstead, L. F. Barcellos, R. Ravindrarajah, R. Abraham, L. Alfredsson, K. Ardlie, C. Aubin, A. Baker, K. Baker, S. E. Baranzini, L. Bergamaschi, R. Bergamaschi, A. Bernstein, A. Berthele, M. Boggild, J. P. Bradfield, D. Brassat, S. A. Broadley, D. Buck, H. Butzkueven, R. Capra, W. M. Carroll, P. Cavalla, E. G. Celius, S. Cepok, R. Chiavacci, F. Clerget-Darpoux, K. Clysters, G. Comi, M. Cossburn, I. Cournu-Rebeix, M. B. Cox, W. Cozen, B. A. C. Cree, A. H. Cross, D. Cusi, M. J. Daly, E. Davis, P. I. W. de Bakker, M. Debouverie, M. B. D'hooghe, K. Dixon, R. Dobosi, B. Dubois, D. Ellinghaus, I. Elovaara, F. Esposito, C. Fontenille, S. Foote, A. Franke, D. Galimberti, A. Ghezzi, J. Glessner, R. Gomez, O. Gout, C. Graham, S. F. A. Grant, F. R. Guerini, H. Hakonarson, P. Hall, A. Hamsten, H.-P. Hartung, R. N. Heard, S. Heath, J. Hobart, M. Hoshi, C. Infante-Duarte, G. Ingram, W. Ingram, T. Islam, M. Jagodic, M. Kabesch, A. G. Kermode, T. J. Kilpatrick, C. Kim, N. Klopp, K. Koivisto, M. Larsson, M. Lathrop, J. S. Lechner-Scott, M. A. Leone, V. Leppä, U. Liljedahl, I. L. Bomfim, R. R. Lincoln, J. Link, J. Liu, A. R. Lorentzen, S. Lupoli, F. Macciardi, T. Mack, M. Marriott, V. Martinelli, D. Mason, J. L. McCauley, F. Mentch, I.-L. Mero, T. Mihalova, X. Montalban, J. Mottershead, K.-M. Myhr, P. Naldi, W. Ollier, A. Page, A. Palotie, J. Pelletier, L. Piccio, T. Pickersgill, F. Piehl, S. Pobywajlo, H. L. Quach, P. P. Ramsay, M. Reunanen, R. Reynolds, J. D. Rioux, M. Rodegher, S. Roesner, J. P. Rubio, I.-M. Rückert, M. Salvetti, E. Salvi, A. Santaniello, C. A. Schaefer, S. Schreiber, C. Schulze, R. J. Scott, F. Sellebjerg, K. W. Selmaj, D. Sexton, L. Shen, B. Simms-Acuna, S. Skidmore, P. M. A. Sleiman, C. Smestad, P. S. Sørensen, H. B. Søndergaard, J. Stankovich, R. C. Strange, A.-M. Sulonen, E. Sundqvist, A.-C. Syvänen, F. Taddeo, B. Taylor, J. M. Blackwell, P. Tienari, E. Bramon, A. Tourbah, M. A. Brown, E. Tronczynska, J. P. Casas, N. Tubridy, A. Corvin, J. Vickery, J. Jankowski, P. Villoslada, H. S. Markus, K. Wang, C. G. Mathew, J. Wason, C. N. A. Palmer, H.-E. Wichmann, R. Plomin, E. Willoughby, A. Rautanen, J. Winkelmann, M. Wittig, R. C. Trembath, J. Yaouanq, A. C. Viswanathan, H. Zhang, N. W. Wood, R. Zuvich, P. Deloukas, C. Langford, A. Duncanson, J. R. Oksenberg, M. A. Pericak-Vance, J. L. Haines, T. Olsson, J. Hillert, A. J. Ivinson, P. L. De Jager, L. Peltonen, G. J. Stewart, D. A. Hafler, S. L. Hauser, G. McVean, P. Donnelly, and A. Compston. 2011. Genetic risk and a primary role for cell-mediated immune mechanisms in multiple sclerosis. *Nature* 476: 214–219.

75. Lindsten, T., C. H. June, and C. B. Thompson. 1988. Multiple mechanisms regulate c-myc gene expression during normal T cell activation. *EMBO J.* 7: 2787–2794.

Figures and Figure Legends.

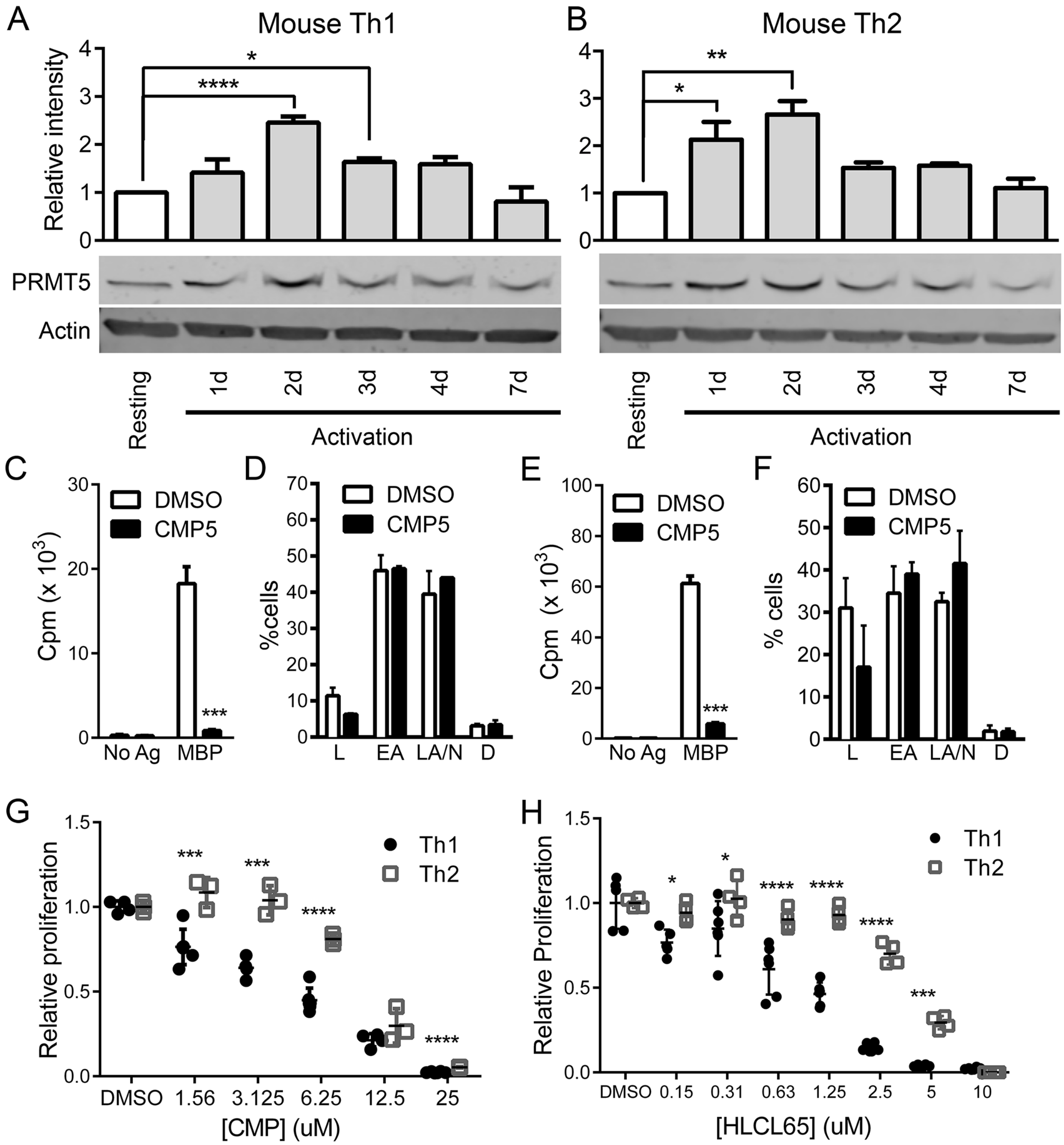

Figure 1. Proliferating murine Th1 and Th2 T cells express increased PRMT5 protein levels. (A-B) Myelin Basic Protein$_{Ac1-11}$ (MBP)-specific T cell receptor (TCR) transgenic (tg) memory Th1 (**A**) and Th2 (**B**) cells were lysed at resting, 1, 2, 3, 4 or 7 days after anti-CD3/CD28 stimulation and analyzed for PRMT5 protein expression by Western blotting.

Resting cells were non-proliferating T cells and were collected 7-10 days after activation of the Th cell line with MBP$_{Ac1-11}$ and irradiated splenocytes. β-actin was used as a loading control. Relative intensity quantification data is shown above a representative blot and was determined by normalizing PRMT5 expression to β-actin expression using ImageStudio. Data is representative of 3-4 independent experiments (n=5 for experiment shown). (One-way ANOVA followed by Sidak's multiple comparison-adjusted t test). (**C-F**) MBP-TCR Tg memory Th1(**C-D**) and Th2 (**E-F**) cells were stimulated with MBP$_{Ac1-11}$ for 48 hours in the presence of the PRMT5 inhibitor CMP5 or vehicle control (DMSO) and proliferation (**C, E**) and viability (**D, F**) were measured by ^{3}H-thymidine incorporation or Annexin V staining, respectively. (Student's t test). Data representative of 3-4 experiments (shown experiment n=4). L: live; EA: early apoptotic, LA: late apoptotic, N: necrotic, D: dead. Data pooled from 2 independent experiments (n=4). (**G-H**) MBP-TCR Tg memory Th1 and Th2 cells were stimulated with anti-CD3/CD28 for 48 hours in the presence of various concentrations of PRMT5 inhibitors CMP5 (**G**), HLCL65 (**H**), or vehicle control. Proliferation was monitored via ^{3}H-thymidine incorporation. (Two-way ANOVA followed by Sidak's multiple comparison adjusted t test). Data representative of 3-4 independent experiments (shown experiment n=4). * $p<0.05$, ** $p< 0.01$, *** $p<0.001$, **** $p< 0.001$

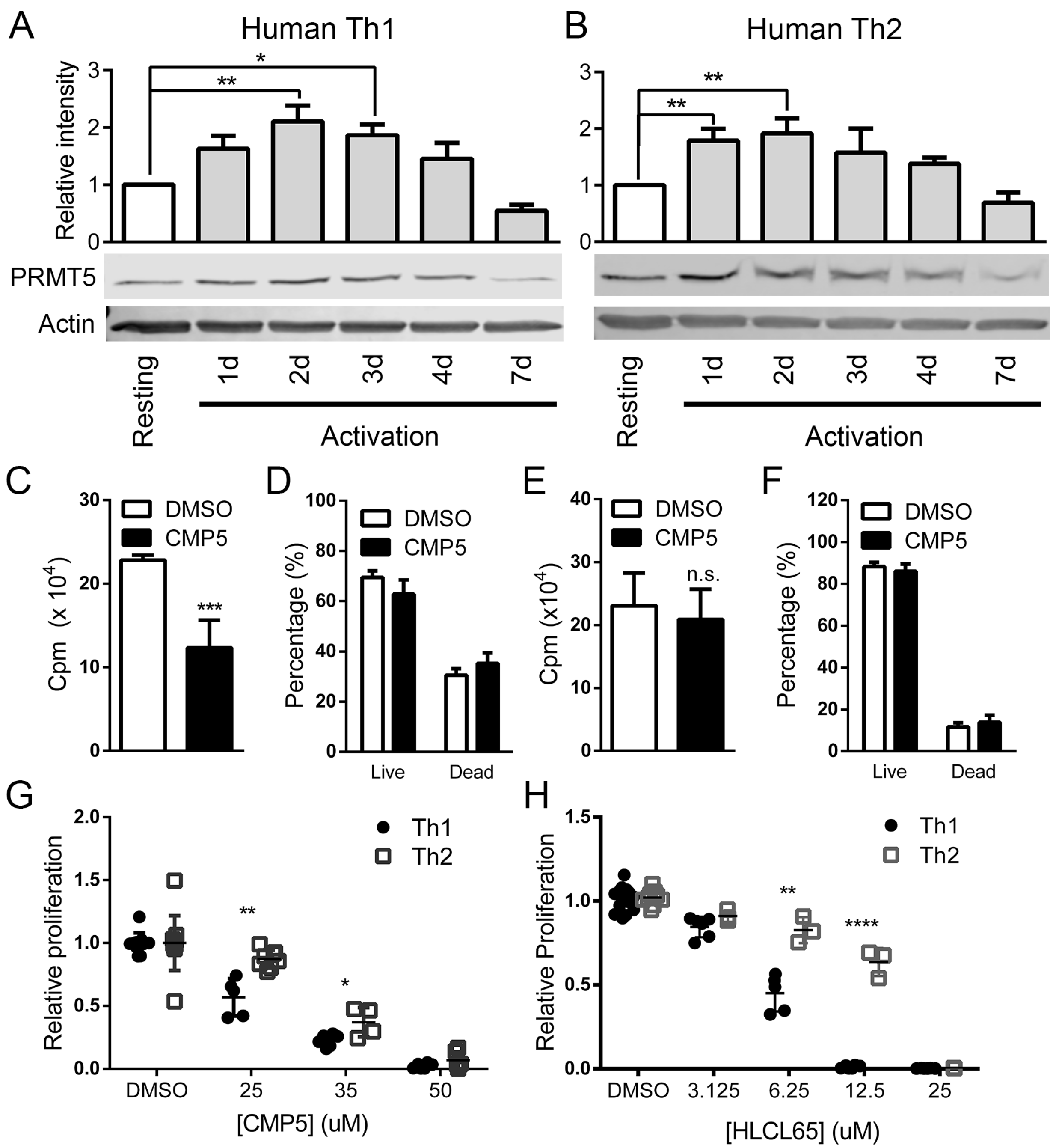

Figure 2. PRMT5 is essential for human Th1 and Th2 cell expansion. Human CD4^{+} T cells were isolated from whole blood and differentiated in the presence of Th1- or Th2- inducing conditions. **(A-B)** After differentiation, Th1 **(A)** and Th2 **(B)** cells were reactivated on anti-CD3/CD28 and cells were lysed at resting, 1, 2, 3, 4 and 7 days. PRMT5 protein expression was analyzed by Western blotting and β-actin was used as a loading control. Relative intensity

quantification data is shown above a representative blot. Data is representative of 3 independent experiments (n=3 for experiment shown). (One-way ANOVA followed by Sidak's multiple comparison-adjusted t test). **(C-F)** Human memory Th1 **(C, D)** and Th2 **(E, F)** T cells were activated with anti-CD3/CD28 for 48 hours in the presence of the PRMT5 inhibitor CMP5 or vehicle control (DMSO) and the extent of T cell expansion (**C, E**) or viability (**D, F**) was measured by ^{3}H-thymidine incorporation or Trypan blue exclusion, respectively. (Student's t test). Data representative of 3-4 experiments (shown experiment n=3). **(G-H)** Human memory Th1 and Th2 cells were activated, as in C-F, in the presence of varying concentrations of vehicle control, CMP5 (**G**), or HLCL65 (**H**) and T cell proliferation was measured by ^{3}H-thymidine incorporation. (Two-way ANOVA followed by Sidak's multiple comparison adjusted t test). * p<0.05, ** p<0.01, *** p<0.001, **** p<0.0001, n.s. =not significant

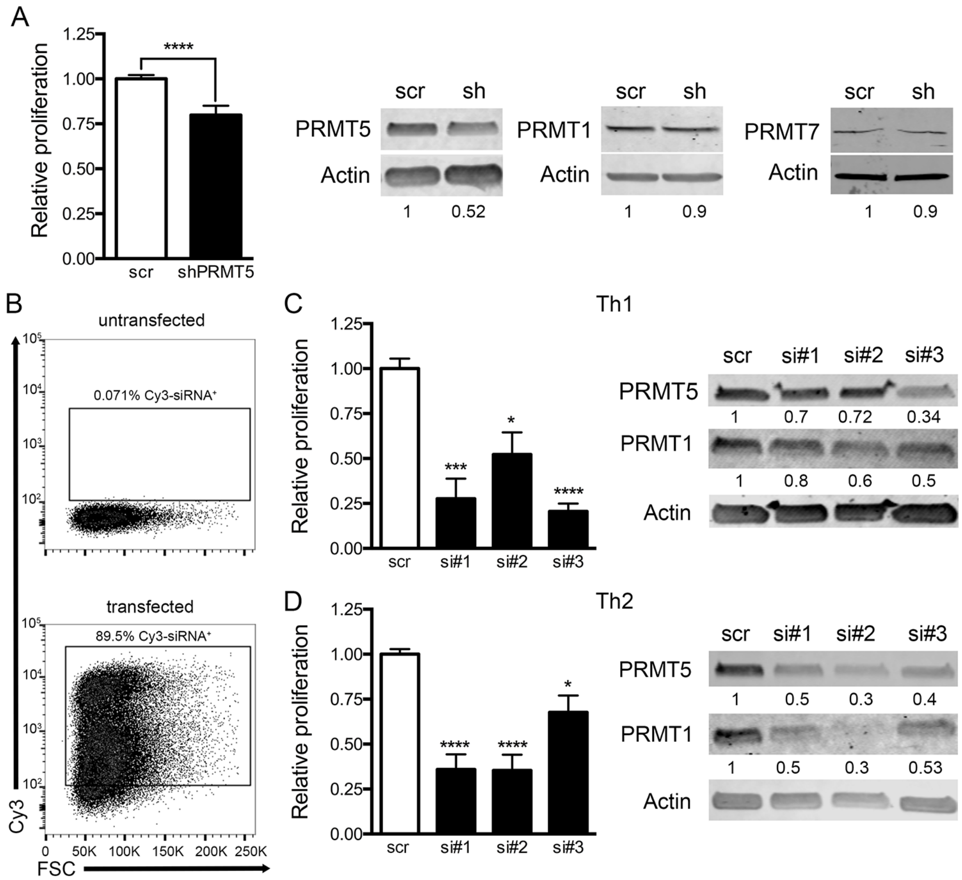

Figure 3. PRMT5 knockdown suppresses human T cell proliferation.

A. Human memory Th1 cells were activated with anti-CD3/CD28 for 48 hours in the presence of PRMT5 short hairpin RNA or scrambled (scr) control and proliferation was monitored via ^{3}H-thymidine incorporation. Left panel shows proliferation, relative to the scrambled control condition (data pooled from 3 independent experiments, Student's t test, n=8). Right panels show PRMT5, PRMT1 and PRMT7 expression measured by Western blot and quantified using ImageStudio software. (**B-D**) Human Th1 and Th2 cells were activated as in **A** in the presence of a Cy3-labeled NS siRNA, nonsense siRNA control (NS) or three different PRMT5-specific siRNAs (si#1-3). (**B**) Cy3siRNA^{+} cells (gated on CD4^{+} cells) were quantified by flow cytometry as a measure of transfection efficiency. The tranfection efficiency shown corresponds to Th1 cells. Equivalent efficiency was observed in Th2 cells. (**C-D**) Proliferation of human Th1 (**C**) and Th2 (**D**) cells was monitored by ^{3}H-thymidine incorporation and expressed as a relative proliferation ratio to proliferation in the NS tranfection control condition. PRMT5 and PRMT1 protein expression was measured by Western blot and quantified using ImageStudio Software (One-way ANOVA followed by Sidak's multiple comparison-adjusted t test). Protein data is representative of three independent experiments. Proliferation data is pooled from three independent experiments (shown n=9). * $p<0.05$, ** $p<0.01$, *** $p<0.001$, **** $p<0.0001$, n.s. =not significant

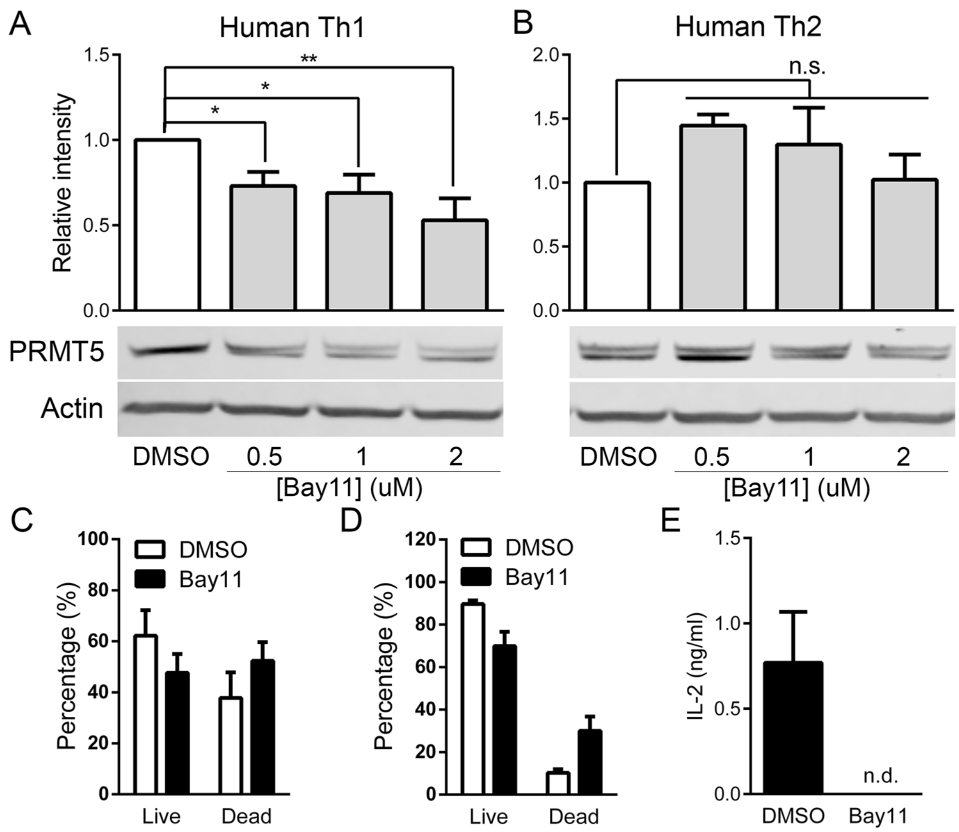

Figure 4. T cell activation drives PRMT5 expression in an NF-κB-dependent manner. Differentiated human Th1 **(A)** or Th2 **(B)** cells were reactivated on anti-CD3/CD28, treated with DMSO vehicle or increasing amounts of the NF-κB pathway inhibitor Bay11-7082 for 8 hrs. Cells were lysed for Western blot analysis of PRMT5 expression 48 hours after initial activation. β-actin was used as a loading control. Relative intensity quantification data is shown above a representative blot quantified with ImageStudio. Data is representative of 3 independent experiments (n=3 for experiment shown). (One-way ANOVA followed by Sidak's multiple comparison-adjusted t test). **(C-D)** Differentiated human Th1 (**C**) and Th2 (**D**) cells were treated as described in A-B and viability was monitored by Trypan blue exclusion. (Two-way ANOVA followed by Sidak's multiple comparison-adjusted t test). Data was pooled from 3 independent experiments (n=6). (**E)** Differentiated human Th1 cells were treated as described in **A** and supernatants were collected to analyze the concentration of IL-2 production by ELISA. Data representative of 3 independent experiments (n=2) * $p<0.05$, ** $p< 0.01$, *** $p<0.001$

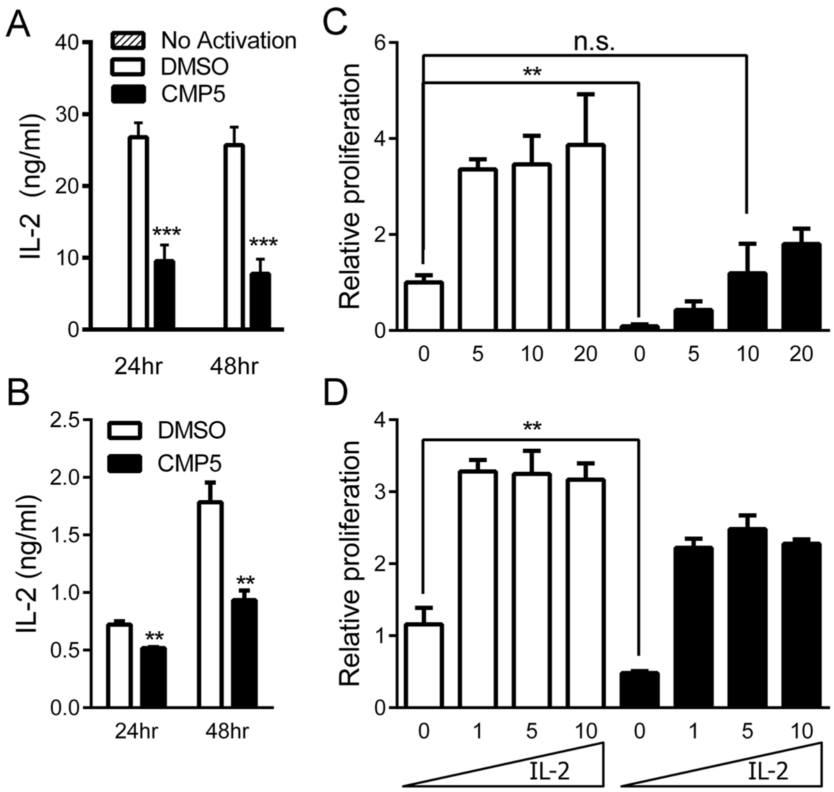

Figure 5. PRMT5 inhibition suppresses IL-2 production and exogenous IL-2 rescues CMP5-inhibited Th cell proliferation. (A) IL-2 measured by an Enzyme Linked Immunosorbent Assay (ELISA) in supernatants of murine MBP TCR Th1 memory T cells **(A)** or human Th1 cells **(B)** stimulated through the TCR at various time-points in the presence of CMP5 or vehicle control. Th2 cells not shown since they do not secrete IL-2. (Student's t test). Data from 2-3 independent experiments (n=4). **(C-D)** Proliferation at 48 hours, measured by ^{3}H-thymidine incorporation, of mouse memory MBP TCR tg Th1 (**C**) or human memory Th1 **(D)** T cells activated with anti-CD3/CD28 in the presence of CMP5 or vehicle control and increasing amounts of exogenous IL-2 (ng/ml). (ANOVA followed by Sidak's multiple comparison-adjusted t test). Data representative of 2-3 independent experiments (shown experiment n=3). * p<0.05, ** p<0.01, *** p<0.001, **** p<0.0001, n.s. =not significant

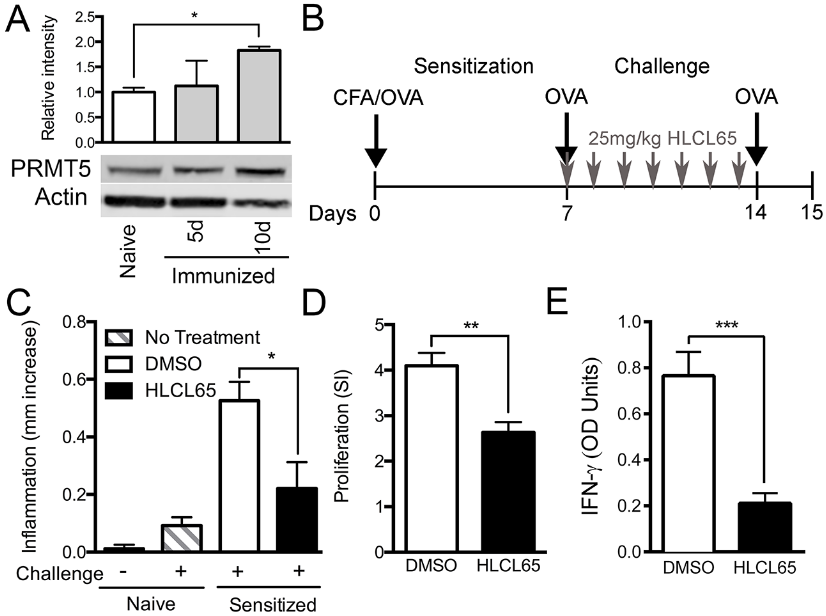

Figure 6. PRMT5 inhibition suppresses T cell responses and inflammation in the Delayed-Type Hypersensitivity model.

(**A**) PRMT5 expression in mouse spleens from naïve mice and 5 or 10 days after immunization with Ovalbumin (OVA) and Complete Freund's Adjuvant (CFA). Spleens were crushed under liquid nitrogen and lysed for Western blot analysis using β-actin as a loading control. Data representative of 2 independent experiments (data shown n=3) (**B**) Schematic of delayed-type hypersensitivity (DTH) model and treatment strategy. Mice were sensitized to OVA with Complete Freund's Adjuvant (CFA)/OVA immunization (flanks and tail base). 7 and 14 days later, mice were footpad challenged with OVA and daily treated intraperitoneally with 25mg/kg PRMT5 inhibitor HLCL65 or DMSO between day 7 and 14. (**C**) Inflammation was evaluated on day 15 after initial sensitization using calipers to quantify footpad swelling. (**D**) Day 15 splenocytes were activated in the presence or absence of OVA for 72 hours and proliferation was monitored by ^{3}H-thymidine incorporation. (**E**) Supernatants were collected from splenocytes isolated as described in **C**, and interferon-gamma production was measured by ELISA. (n=8). Data representative of 2 independent experiments.

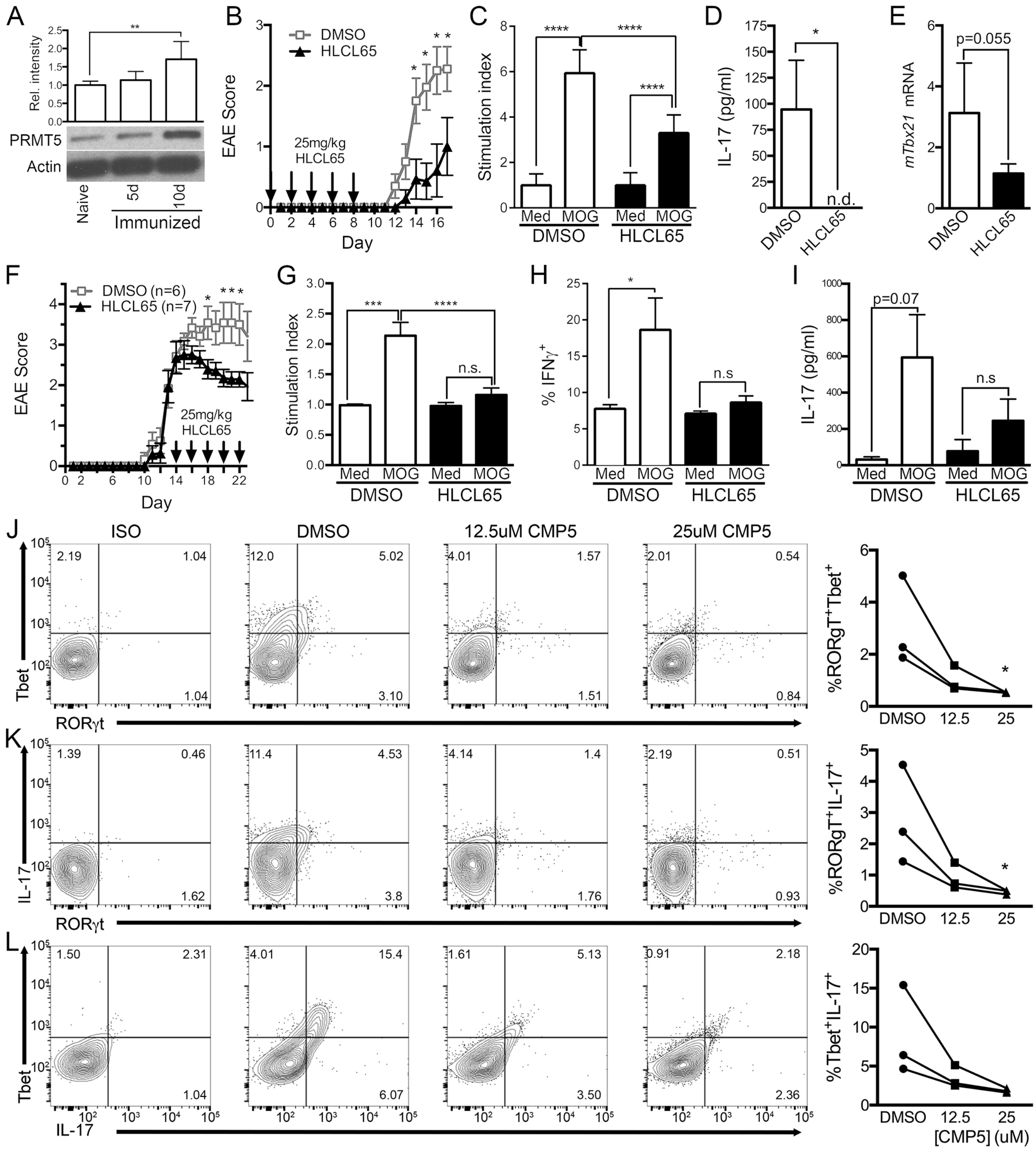

1017

1018 **Figure 7. PRMT5 inhibition suppresses *in vivo* inflammatory T cell responses and clinical**

1019 **disease in the Experimental Autoimmune Encephalomyelitis (EAE) murine model of**

1020 **Multiple Sclerosis.**

(**A**) PRMT5 expression in mouse spleens from naïve mice, 5 or 10 days after immunization with CFA/Myelin Oligodendrocyte Glycoprotein (MOG) in the preclinical EAE phase. Spleens were crushed under liquid nitrogen and lysed for Western blot analysis using β-actin as a loading control. Representative data of 2 independent experiments (n=4). (**B**) Clinical EAE score in mice preventatively treated with DMSO vehicle or 25mg/kg HLCL65 (q.o.d., arrows indicate treatment) from days 0-9 after CFA/MOG immunization to induce EAE (n=10). EAE score (**B**) and day of onset were blindly monitored daily. (**C-D**) Splenocytes (**C**) and brain/spinal cord mononuclear cells (**D**) were isolated from DMSO or HLCL65-treated mice and activated in the presence or absence of MOG 35-55. MOG-specific proliferation (**C**) was monitored via ^{3}H-thymidine incorporation (One-way ANOVA followed by Sidak's multiple comparison adjusted t test, n=3). MOG-specific IL-17 production (**D**) was measured by ELISA (Student's t test, n=2 samples each pooled from 6 individual mice/group). (**E**) RNA was isolated from brains and spinal cord homogenates of DMSO or HLCL65-treated mice and *Tbx21* mRNA expression was measured by qRT-PCR (Student's t test, n=6). (**F**) EAE in mice treated with DMSO vehicle or 25mg/kg HLCL65 (q.o.d., arrows indicate treatment) starting on day 14 post-immunization, after EAE developed. Mice were randomly assigned to either group (pre-treatment average score were 1.92 for DMSO and 1.96 for HLCL65 group) and blindly scored for EAE daily. (n=6-7). (**G-I**) Mice were CFA/MOG immunized and treated with DMSO or 25mg/kg HLCL65 every other day starting 1 week after immunization. Splenocytes were isolated from DMSO or HLCL65-treated mice 10 days after immunization and activated in the presence or absence of MOG. MOG-specific proliferation was monitored via ^{3}H-thymidine incorporation (**G**), IFNγ$^+$-secreting cells were quantified by flow cytometry (gated on CD4$^+$, CD44$^+$ cells) (**H**), and IL-17 production was measured by ELISA (**I**). (One-Way ANOVA followed by Sidak's multiple comparison-adjusted t test). (**J-L**) Splenocytes were isolated from MBP TCR Tg mice with spontaneous EAE, activated with MBPAc1-11 in the presence of with the indicated concentrations of PRMT5 inhibitors CMP5 and HLCL65, or DMSO vehicle control for 48hrs. Frequencies of RORγt$^+$Tbet$^+$ (**J**), RORγt$^+$IL-17$^+$ (**K**), and IL-17$^+$Tbet$^+$ (**L**) T cells were quantified by intracellular flow cytometry on a CD4$^+$CD44$^+$ T cell gate. * p<0.05, ** p<0.01, *** p<0.001, **** p<0.0001.

Supplemental Figure 1.

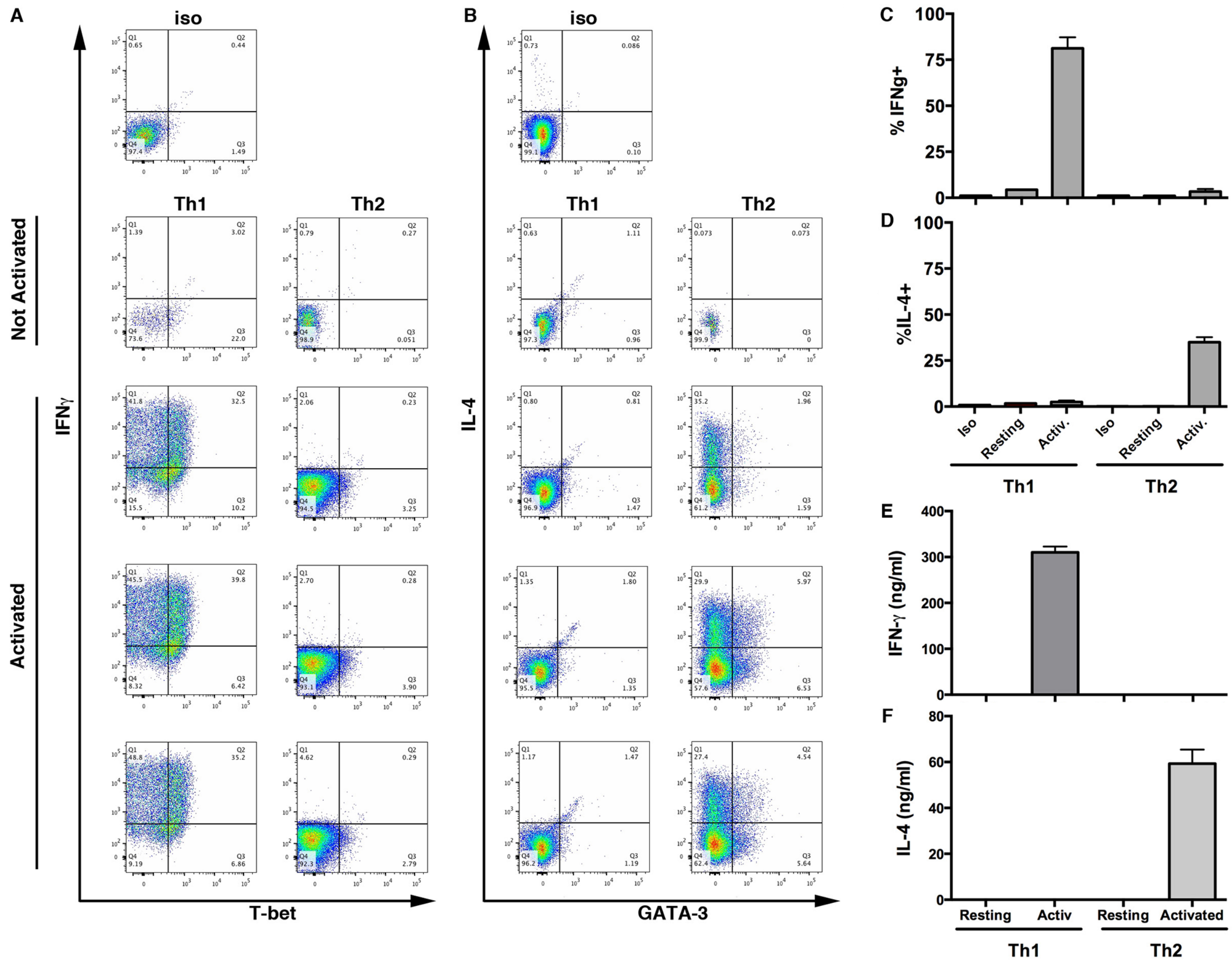

Supplemental Figure 1. Characterization of Myelin Basic Protein (MBP) Ac$_{1\text{-}11}$ TcR transgenic (Tg) Th1 and Th2 cell lines.

IFN-γ and T-bet (**A**) and IL-4 and GATA-3 (**B**) flow cytometry analysis of MBP TcR Tg Th1 and Th2 cell lines activated for 48 hours with anti-CD3/CD28. Cells were treated with transport inhibitor GolgiPlug for the last four hours of culture. The percentage of cytokine positive cells from **A** and **B** is quantified in **C** (IFN-γ^+ cells) and **D** (IL-4^+ cells). Flow data was from one experiment (n=3) representative of three independent experiments. The amount of secreted IFN-γ (**E**) and IL-4 (**F**) was quantified by ELISA on supernatants from MBP TcR Tg Th1 and Th2 cell lines activated on anti-CD3/CD28 for 48 hours. ELISA data is from one experiment (n=3) representative of three independent experiments.

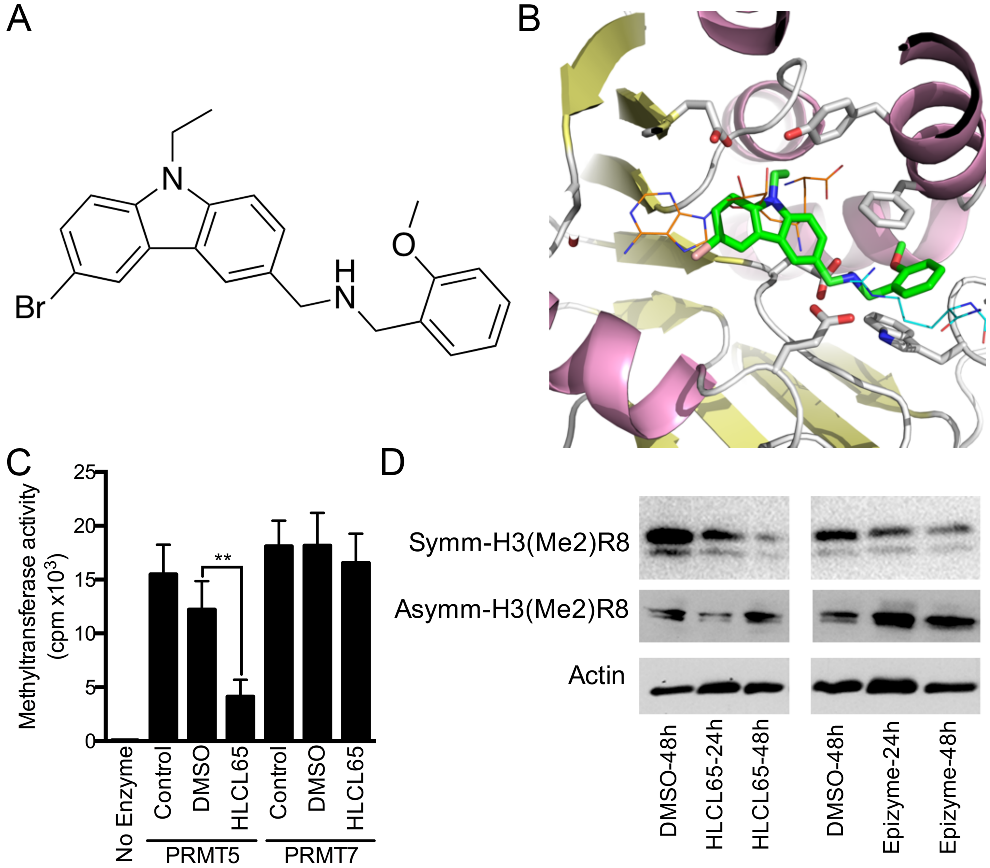

Supplemental Figure 2. Characterization of Second Generation PRMT5 inhibitor, HLCL65.

(**A**) Chemical structure of HLCL65. (**B**) The PRMT5 binding pocket is shown as cartoon (PDB 4GQB), α-helix, β-sheets and turns are colored pink, yellow and grey, respectively. The bound SAM analog (A9145C) is shown in orange, and the H4 peptide with substrate residue Arg3 is shown in cyan as lines. Docked HLCL65 molecule is represented by sticks in green.

(**C**) Histone methyltransferase assays were performed by incubating H1-depleted HeLa-core histones (2 µg) with affinity-purified hSWI/SNF associated Fl-PRMT5, or Fl-PRMT7 in the presence of [^{3}H]AdoMet and control DMSO or 20uM of HLCL65. Reaction samples were spotted onto Whatman P-81 filter paper before methylation of histone was quantified by liquid scintillation counting. Each reaction was done in triplicate. (**D**) CCMCL1 cell lines were treated with 20uM of HLCL65, 20 uM of Epizyme compound for 24h or 48h, and RIPA extracts (40 μg) were analyzed for Symm-H3(Me2)R8 or asymm-H3(Me2)R8 protein levels. Actin was used as loading control. * $p<0.05$, ** $p<0.01$, *** $p<0.001$, **** $p<0.0001$

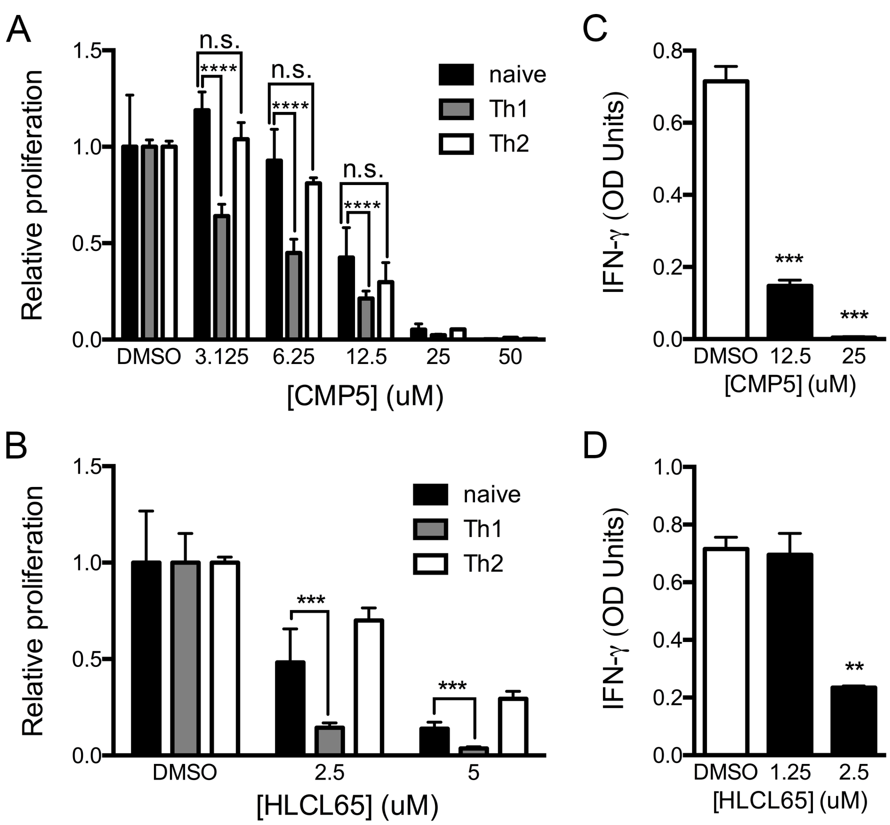

Supplemental Figure 3. PRMT5 inhibitors suppress naïve T cell proliferation less potently than inflammatory memory Th1 cell responses.

(**A-D**) Naïve $CD4^+$ T cells were isolated from splenocytes, activated on anti-CD3/CD28 and treated in the presence of DMSO vehicle control, CMP5 (**A, C**), or HLCL65 (**B, D**). At 48 hours, proliferation was monitored by ^{3}H-thymidine incorporation (**A-B**) and IFNγ production was quantified by ELISA (**C-D**).

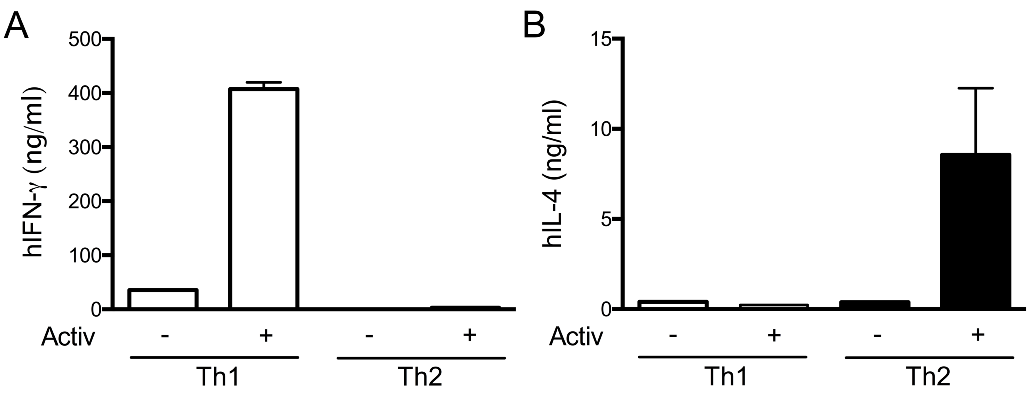

Supplemental Figure 4. Characterization of Human Th1- and Th2-enriched Cells.

The amount of production of IFN-γ (**A**) and IL-4 (**B**) was quantified by ELISA of the supernatants from normal donor human Th1- and Th2-enriched cells activated for 24 hours with anti-CD3/CD28. Data is representative of three independent experiments (n=2).

Tables

	Cell Type	IC_{50} (uM)	Hill Slope	R-squared
CMP5	mTh1	3.7	-0.8334	0.96
	mTh2	9.2	-3.174	0.98
	hTh1	26.9	-3.454	0.94
	hTh2	31.6	-6.276	0.96
HLCL65	mTh1	1.1	-1.392	0.91
	mTh2	4	-2.321	0.97
	hTh1	5.7	-3.291	0.98
	hTh2	14.3	-4.15	0.97

Table 1. IC_{50} values for PRMT5 inhibitors CMP5 and HLCL65 in mouse and human Th1 and Th2 cells.

IC_{50}, Hill Slope, and R^2 values reported for PRMT5 inhibitors in Th1 and Th2 cell lines.

	DMSO	HLCL65	Change from DMSO	p-value
EAE incidence (%)	90	57	-33%	N/A
Disease Onset (Days)	13.44 ± 0.53	16.86 ± 0.96	+3.42 days	0.0053
Area under the Curve (AUC)	8.214 ± 1.58	2.143 ± 1.41	-6.071	0.0159
Average Score D17	2.3 ± 0.37	1.0 ± 0.48	-1.3	0.048
Average Max Score	2.45 ± 0.37	1.0 ± 0.48	-1.45	0.0285
n	10	7	n/a	n/a

Table 2. Prophylactic treatment with HLCL65 ameliorates EAE.

Mean ± standard deviation for characteristics of EAE in mice treated with DMSO or HLCL65 in a preventative model.

	DMSO	HLCL65	Change from DMSO	p-value
EAE Incidence (%): pre Tx	100	100	0	N/A
Disease Onset (Days): pre Tx	11.67 ± 0.49	12.43 ± 0.37	+0.76 days	n.s.
Average Score D14*	2.7 ± 0.40	2.7 ± 0.40	0	n.s.
Area Under the Curve (AUC): pre Tx	4.60 ± 1.15	3.91 ± 0.91	-0.69	n.s.
Area Under the Curve (AUC): post Tx	27.31 ± 3.13	19.11 ± 1.61	-8.2	0.0329
Average Max Score: pre Tx	2.7 ± 0.40	2.7 ± 0.40	0	n.s.
Average Max Score: post Tx	3.88 ± 0.38	2.93 ± 0.44	-0.95	0.0535
Average Score D22	3.5 ± 0.51	2.14 ± 0.19	-1.36	0.0228
n	6	7	n/a	n/a

Table 3. Therapeutic treatment with HLCL65 ameliorates EAE.

Mean ± standard deviation for characteristics of EAE in mice treated with DMSO or HLCL65 in a therapeutic model. Tx = treatment. *Treatment initiation occurred on day 14.